Development of a calibration unit for an Interstitial Photodynamic Therapy system

Master's Thesis
by
Johan Axelsson and Johan Stensson

Lund Reports on Atomic Physics, LRAP-335
Lund, December 2004

Abstract

Interstitial photodynamic therapy (IPDT) is the cancer treatment modality of inserting optical fibers into a tumor for delivering laser light to activate an accumulated medical substance. An IPDT system has been developed by the Atomic Physics Division at Lund University, Sweden, and is subject to clinical trials. The system not only carries out delivery of the therapeutic irradiation using a set of optical fibers inserted into the tumor mass, but also monitors properties of the tumor tissue using the same optical fibers to collect light. Due to varying transmission losses in the optical fiber couplings, a calibration has to be made before each treatment session, both for emitted laser power and measurement capability.

This thesis describes the work of designing and constructing a first prototype for a calibration unit. Several solutions were considered and evaluated before deciding on a final design. A prototype was then built and evaluated.

Table of contents

ABBREVIATIONS AND ACRONYMS

1. INTRODUCTION 1

2. PHOTODYNAMIC THERAPY 2

2.1. MEDICAL BACKGROUND OF PDT 2
2.2. LIGHT TRANSPORT IN TISSUE 3
2.2.1. ABSORPTION 3
2.2.2. SCATTERING 3
2.2.3. TISSUE OPTICAL PROPERTIES 4
2.2.4. THEORETICAL MODELING OF LIGHT IN TISSUE 4
2.3. PHOTODYNAMIC REACTION 7
2.3.1. THE REACTION 7
2.3.2. LIGHT 8
2.3.3. OXYGEN 8
2.4. PHOTOSENSITIZER 8
2.4.1. HPD AND PHOTOFRIN 9
2.4.2. ALA 9
2.4.3. FOSCAN 9
2.5. CLINICAL ASPECTS OF PDT 10
2.5.1. TUMOR DAMAGE 10
2.5.2. PHOTOBLEACHING 10
2.5.3. DOSIMETRY 10
2.5.4. INTERSTITIAL PHOTODYNAMIC THERAPY 11

3. INTERSTITIAL PHOTODYNAMIC THERAPY SYSTEM 12

3.1. TREATMENT SESSION 12
3.1.1. PREPARATION 12
3.1.2. TREATMENT 13
3.2. SYSTEM OUTLINE 14
3.2.1. LASER DIODES 14
3.2.2. FIBER COUPLED LIGHT DIVIDER 14
3.2.3. OPTICAL FIBERS 15
3.3. THERAPEUTICS WITH THE IPDT SYSTEM 16
3.3.1. TREATMENT MODE 16
3.3.2. DIAGNOSTIC MODE 17
3.3.2.1. Fluence rate 18
3.3.2.2. Photosensitizer concentration 18
3.3.2.3. Oxygen saturation level 18
3.4. SYSTEM LOSSES AND THE NEED FOR CALIBRATION 19
3.5. FIBER HOLDER 19

4. CALIBRATION ALTERNATIVES 20

4.1. TREATMENT MODE 20
4.1.1. INTEGRATING SPHERE 20
4.1.1.1. What is an integrating sphere? 20
4.1.1.2. General idea 21
4.1.1.3. Problems 22
4.1.2. PHOTODIODE 22
4.1.2.1. What is a photodiode? 22
4.1.2.2. General idea 22
4.1.2.3. Measurements 22
4.1.2.4. Problems 23
4.2. DIAGNOSTIC MODE 23
4.2.1. DETECTED POWER INTERVAL 24
4.2.2. TISSUE PHANTOM 25

4.2.2.1. What is a tissue phantom? 25
4.2.2.2. General idea 26
4.2.2.3. Problems 26
4.2.3. INTEGRATING SPHERE 27
4.2.3.1. General idea 27
4.2.3.2. Problems 28
4.2.4. DIFFUSE TRANSMITTANCE 28
4.2.4.1. General idea 28
4.2.4.2. Measurements 29
4.2.4.3. Problems 30
4.2.5. DIFFUSE REFLECTANCE 31
4.2.5.1. General idea 31
4.2.5.2. Measurements 33
4.2.5.3. Problems 35
4.3. CALIBRATION ALTERNATIVE SELECTION 36
4.3.1. TREATMENT MODE 36
4.3.2. DIAGNOSTIC MODE 36

5. CALIBRATION UNIT IMPLEMENTATION 37

5.1. PROTOTYPE CONSTRUCTION 37
5.1.1. THE SLED 37
5.1.1.1. Station 2 (Photodiode) 38
5.1.1.2. Station 3 (Offset) 38
5.1.1.3. Station 4 (Diffuser) 39
5.1.2. BOX SIZE 39
5.1.3. DESIGNING THE REFLECTOR BLOCKER 39
5.1.4. FIBER HOLDER CONSTRUCTION 40
5.2. PROGRAMMING 41
5.2.1. TREATMENT MODE 42
5.2.2. DIAGNOSTIC MODE 42

6. PROTOTYPE EVALUATION 43

6.1. EXPERIMENTAL RESULTS 43
6.1.1. PHOTODIODE LIGHT CONE ACCEPTANCE 44
6.1.2. DIFFUSE REFLECTANCE UNIFORMITY 45
6.1.2.1. Light leakage 45
6.1.2.2. Reflector blocker material 46
6.1.2.3. Fiber alignment 47
6.2. CALIBRATION SESSION 48

7. DISCUSSION 50

8. FUTURE WORK 51

9. ACKNOWLEDGEMENTS 52

10. REFERENCES 53

APPENDIX A A-1

RADIOMETRIC DEFINITIONS A-1
RADIANCE A-1
FLUENCE RATE A-1
RADIANT POWER A-2
RADIANT INTENSITY A-2
IRRADIANCE A-2

APPENDIX B B-1

PROTOTYPE EVALUATION MEASUREMENT RESULTS B-1

Abbreviations and acronyms

ALA	δ-aminolaevulinic acid
HbO_2	oxygenated haemoglobin
Hb	de-oxygenated haemoglobin
HpD	haematoporphyrin derivative
IPDT	interstitial photodynamic therapy
IR	infrared
LED	light emitting diode
LD	laser diode
mTHPC	meta-tetrahydrophenylchlorin, also Foscan®
NIR	near infrared
PDT	photodynamic therapy
PpIx	protoporphyrin IX
S_{O2}	oxygen saturation level

1. Introduction

Cancer is a growing and varied disease that affects most of us, either in the form of ourselves being struck by it or someone close to us. Most old men suffer from a benign enlarged prostatic gland and about one tenth of all men will have malign cancer tumor growth, prostate cancer. Photodynamic therapy offers a method of treatment without the drawbacks of treatment modalities used clinically today, such as radiation and chemical therapy. Photodynamic therapy uses light to activate a chemical compound absorbed by the tumor cells, causing the tumor tissue to be destroyed.

The Atomic Physics Division at Lund University has together with SpectraCure AB, Sweden, developed an interstitial photodynamic therapy (IPDT) system capable of treating cancer patients using optical fibers for light delivery.

When treating a patient one has to know how much light is delivered into the tumor. The system is also capable of monitoring certain properties during treatment. This is done by analyzing the light transmission between patient fibers. Since all optical systems introduce losses the IPDT system has to be calibrated to know how much light is detected and how much light is delivered. This calibration should be done in a clinical environment prior to the treatment session. Thus the calibration should be user-friendly and preferably automatic.

This Master's Thesis aims to be a development of a first prototype of a calibration unit to be used with SpectraCure's IPDT system. Several different technical solutions were considered and experimented with until the final design proposed in this report was decided on. A fiber holder was also designed.

The thesis gives a brief introduction to tissue optics and the basics of photodynamic therapy in Chapter 2. The IPDT system is then described in Chapter 3. Chapter 4 discusses several calibration alternatives and is concluded by a selection of alternative. In Chapter 5 the implementation of the selected alternative is described and in Chapter 6 the calibration unit is evaluated. Discussion and proposal of future work concludes the thesis in Chapter 7 and Chapter 8.

particle is larger than the wavelength Mie theory should be used. The number of scattering events induced by a Rayleigh scatterer is proportional to λ^{-4}. The wavelength dependence for a Mie scatterer follows λ^{-2}. Biological tissue displays scattering characteristics that is a mixture of Rayleigh and Mie scattering. Due to this, blue light is more scattered than red light as seen in Figure 2-2.[7]

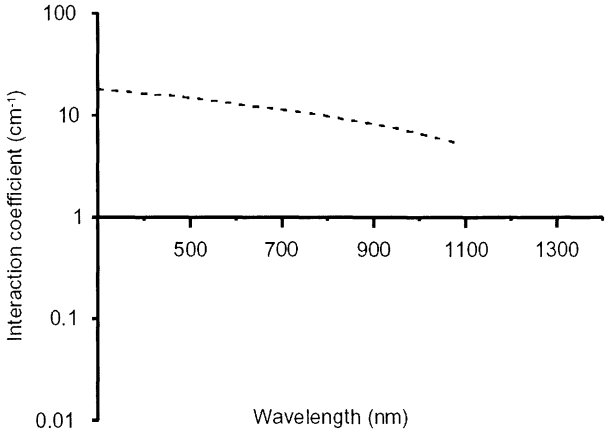

Figure 2-2. Typical scattering coefficient for tissue as a function of wavelength.[7]

The scattering process is anisotropic, which means that the probability of scattering is not equal in all directions. There is a larger probability for the light to be scattered in the forward direction than in the backward direction.

2.2.3. Tissue optical properties

Tissue is built up of different biological molecules, which are able to absorb and scatter light. To simplify, tissue can often be seen as a homogenous medium with constant absorbing and scattering properties. Three properties are used to describe tissue;

- The absorption coefficient, μ_a (cm^{-1}), describes the most probable number of absorbing events that occur per unit distance.
- The scattering coefficient, μ_S (cm^{-1}), describes the most probable number of scattering events that occur per unit distance.
- The anisotropy factor, g (-), describes the cosine of the most probable scattering direction of the light.

2.2.4. Theoretical modeling of light in tissue

Simulating light propagation in tissue can be done using the radiative transport equation or Maxwell's equations, in which light propagation is treated as energy transfer by electromagnetic waves. The latter approach is quite complicated when applied to tissue optics. Imagine

the tissue as a collection of particles. If the collection only consists of a few particles far from each other the light distribution is only affected by one particle at a time. The light distribution from each particle can then be added to get the total light distribution. Tissue consists of a large amount of particles and hence the light distribution is perturbed by many particles. This multiple scattering is hard to treat with Maxwell's equations.[8]

A more common way to treat the light propagation in tissue is the radiative transport theory. Here the light is treated as a stream of photons incident on an infinitesimal small volume of tissue. When deriving the transport equation the energy balance equation of incoming, outgoing, absorbed and emitted photons is considered.

Since the radiative transport equation has no analytical solution, approximations and numerical techniques are used to model the light propagation[8]. One way is to use discretization methods such as Kubelka-Munk or Adding-Doubling where the transport equation is reduced to one dimension.

Another approach is to use the probabilistic Monte-Carlo method. Here one photon's path is followed during its way through the tissue. In each step there are certain probabilities for the photon to be absorbed or scattered in different directions.[8]

The last alternative is to use expansion methods where the diffusion approximation is the one most used. To get the diffusion approximation the transport equation is expanded in spherical harmonics. This yields an infinite series of differential equations. The approximation is made by only including the first two terms in the series. The first part describes the collimated part of the light and the second part describes the light from an isotropic source.[7,8]

An optical fiber, delivering the therapeutic light in IPDT, is sometimes approximated as a point source in an infinite homogenous medium in which the diffusion equation can be solved analytically. The solution is:

$$\varphi(r) = \frac{P \cdot \mu_{eff}^2}{4\pi\mu_a} \cdot \frac{1}{|r|} \cdot e^{-\mu_{eff}|r|} \qquad \textit{Equation 2-1}$$

where

φ : fluence rate (W/cm^2), see Appendix A.

r : distance from source (cm)

P : delivered light power (W)

μ_a : absorption coefficient (cm^{-1})

μ_{eff} : effective extinction coefficient (cm^{-1})

The effective extinction coefficient is achieved in the derivation of the diffusion approximation and is defined as:

$$\mu_{eff} = \sqrt{3\mu_a(\mu_a + \mu_s')} \qquad \textit{Equation 2-2}$$

μ_s' is called the reduced scattering coefficients and is defined as:

$$\mu_s' = \mu_s(1-g) \qquad \textit{Equation 2-3}$$

Equation 2-1 can also be solved for a laser beam incident on a tissue surface. The photons will be absorbed and forward scattered. A schematic picture is shown in Figure 2-3a. According to the diffusion approximation this light distribution could be modeled as an isotropic light source at some depth. The depth of the isotropic light source depends on the tissue optical properties. An assumption often used is that all photons scatter initially at a depth equal to the mean free path for effective isotropic scattering, $z_0 = 1/\mu_s'$, see Figure 2-3b. To compensate for the internal reflections occurring at the tissue surface certain boundary conditions have to be introduced. Using the extrapolated boundary approximation a mirrored isotropic point source is introduced above the surface so that the resulting fluence rate is zero at the extrapolated boundary. The extrapolated boundary is an imagined surface slightly above the real tissue surface.

By evaluating Equation 2-1 with the correct tissue optical properties and laser power the fluence rate distribution in the geometry is achieved.[7]

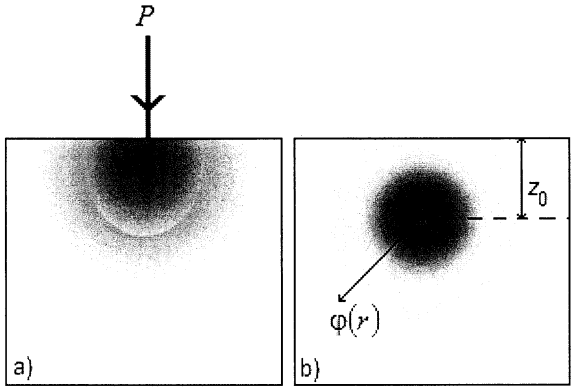

Figure 2-3. a) A schematic figure of the light propagation from an incident light beam. b) An isotropic light source due to the incident light beam[7].

To assure the validity of the diffusion approximation the following restrictions should hold [7]:

- $\mu_s' >> \mu_a$
  This implies that diffusion approximation is only valid when the anisotropy is small.
- The distance between the source and the location where the fluence rate is calculated must be large. The reason is

that the light must undergo a certain amount of scattering events to ascertain a diffuse propagation.

A practical application of the diffusion approximation is calculating the delivered light dose in e.g. interstitial photodynamic therapy.

2.3. *Photodynamic reaction*

The photodynamic reaction is the process that might occur when incident light is absorbed by a chromophore, e.g. a photosensitizer.

2.3.1. The reaction

When the light is absorbed the molecule gains energy. The excess energy gives rise to several different processes. In Figure 2-4 these processes are explained.

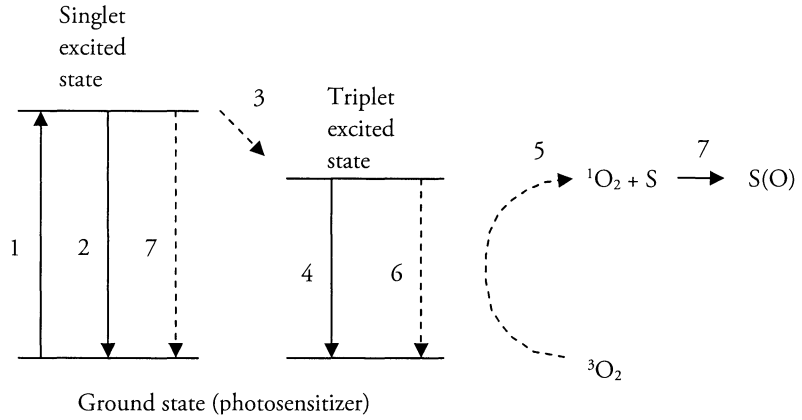

Figure 2-4. Jablonski diagram of different processes that occur when light interacts with photosensitizers in tissue [2].

1. The incoming light is absorbed.
2. The excited molecule can relax to the ground state by emitting fluorescence.
3. The excited molecule can relax to an excited triplet state.
4. The molecule, in excited triplet state, can emit the energy through phosphorescence.
5. The molecule, in excited triplet state, can transfer its energy to surrounding molecules, e.g. molecular oxygen, without emitting radiation.
6. The molecule, in excited triplet state, can collide with surrounding molecules, whereby energy is lost.
7. In an environment where there is oxygen the ground state of oxygen ($^3O_2$) can be excited, described in 5. The excited state of oxygen is called singlet oxygen ($^1O_2$). Due to its highly reactive properties it reacts with surrounding biological molecules, whereby the tissue is damaged.

2.3.2. Light

The start of the photodynamic reaction is the absorption of light, which imposes some requirements for the light. First, the tumor has to receive a certain light dose. Since the light is absorbed and scattered the fluence rate is attenuated while propagating through the tissue. If the power is low the number of photons propagating in the tissue is small and might not be enough for the production of singlet oxygen. If the power delivered to the tissue is too high the tissue cells will vaporize and the selective tumor damage is lost.

Secondly, when the light reaches a chromophore it can only be absorbed if the wavelength matches the energy gap between ground state and excited state of the chromophore[3]. Photodynamic treatment is commonly performed with red light sources due to longer wavelengths being less attenuated than shorter, as described earlier. The light sources most frequently used are lasers, which provide high power density within a specific and narrow wavelength interval. This can be delivered to the tumor site using optical fibers[2].

2.3.3. Oxygen

As pointed out oxygen is fundamental to the photodynamic reaction. If there is no oxygen no reaction will take place. It has been shown that oxygen consumption, during the reaction, increases with the fluence rate of the light[2]. By using lower fluence rates the oxygen is not depleted as fast and singlet oxygen is present during a longer time as new oxygen reaches the tissue via blood circulation. The cost is longer treatment times.

The high reactivity of singlet oxygen induces reactions shortly after the production of singlet oxygen, hence the lifetime is short. The photodynamic reaction is thereby confined to regions close to the absorbing photosensitizer[2].

2.4. Photosensitizer

Photosensitizers are the general name of substances that accumulate in tumor tissue where absorption of light can result in several processes. The natural photosensitizer, accumulated in tumor tissue, is called porphyrin. After this was realized researchers have tried to develop substances with similar properties.[9]

The optimal photosensitizer should accumulate more in tumor tissue than in normal tissue. The photosensitizers light absorption should also be maximized for red wavelengths were the light is not attenuated too much in the tissue. Most photosensitizers have large absorption for wavelengths between 400 and 430 nm and only smaller absorption for wavelengths above 550 nm[1]. Some of the existing photosensitizers will be mentioned here.

2.4.1. HpD and Photofrin

Hematoporphyrin derivate (HpD) is manufactured by preparing hematoporphyrin with acetic and sulphuric acids. Purified HpD is called Photofrin. Photosensitizers based on porphyrins have strong absorption around 400 nm but the absorption peak commonly used in PDT is 632 nm.[7]

These photosensitizers accumulate selectively in the tumor but the time between administration and treatment has to be a couple of days since the accumulation takes some time[1]. The clearance from the body is also slow and PDT with Photofrin is associated with light sensitivity after treatment[7]. Another drawback with these photosensitizers is the short penetration depth, 5-10 mm, of light with wavelength 632 nm. Due to this only small tumor volumes can be treated.

HpD was clinically approved in 1993, in Canada, to be used in PDT of the bladder. Other applications are gastric and lung cancer.[7,1]

2.4.2. ALA

δ-amino levulinic acid, ALA, is a natural occurring substance in the human body. It is one of the precursors to haem which is the red pigment in blood. ALA is transformed to the photoactive compound protoporphyrin IX (PpIX) which continues to form haem. When administered to the body PpIX is produced more extensively in tumor tissue than in normal tissue due to enzyme reactions, a step in the haem cycle that is more active in tumor tissue. A selective accumulation of PpIX is thereby achieved in the tumor.

The absorption peak used in ALA-mediated PDT is 635 nm. PpIX is accumulated faster in tumor tissue compared to HpD and cleared out of the body in one or two days[7].

ALA-mediated PDT is widely used for skin tumors since it can be applied topically as a cream. Applying the photosensitizer selectively is more advantageous than administering it systematically, e.g. by drinking it, since the tumor is targeted more directly[6].

2.4.3. Foscan

mTHPC, Foscan, is one of the most potent photosensitizers of today [1]. Foscan is made of reduced porphyrins, chlorines, which is the same base for forming chlorophyll. The advantage of the chlorines is that the largest absorption peak is in the red region. Foscan absorbs light with wavelength 652 nm, which travels farther than shorter wavelengths before being absorbed, which results in larger treated volumes compared to the above mentioned photosensitizers. Foscan has shown to be an effective photosensitizer in treating head and neck cancer as well as the prostate.[7,1]

2.5. *Clinical aspects of PDT*

As pointed out above the treatment of cancer tumors with PDT demands light, oxygen and a light absorbing pharmaceutical accumulated in the tumor. This will preferably induce tumor damage.

2.5.1. Tumor damage

When singlet oxygen reacts with organic substrates these are destroyed. It has been suggested that the tumor damage in photodynamic therapy is mainly caused by vascular destruction and as a result of this the tumor cells are starved to death, since no oxygen or nutrients are delivered. Other reasons for tumor damage are the destruction of cell membrane by singlet oxygen and reactions inside the tumor cell, such as destruction of DNA and mitochondria[2].

Photosensitizers differ in their tumor destruction mechanisms. ALA gives rise to necrosis and apoptosis[10] (self-programmed cell death) while other sensitizers may work by destroying blood vessels leading to the tumor, making the tumor die from starvation[11].

2.5.2. Photobleaching

If singlet oxygen instead of damaging the tissue oxidizes the photosensitizer, the sensitizer is destroyed and cannot take part in the photodynamic reaction. The concentration of photosensitizer is thus degraded. This is commonly referred to as photobleaching.

Photobleaching is monitored by detecting the fluorescence from the photosensitizer. When the concentration decreases the fluorescence intensity also decreases. [7,2]

It is not evident how photobleaching affects PDT treatment. One suggestion is that photobleaching may rapidly destroy photosensitizer compounds accumulated in the healthy tissue which would increase the selective nature of PDT[2].

Rapidly decreasing photosensitizer fluorescence also indicates that the tissue is well oxygenized[12]. High oxygen concentration in the tissue results in better treatment outcome.

2.5.3. Dosimetry

Dosimetry is essential to the treatment response. The dose delivered to the tumor is defined theoretically as[2]:

$$D_{PDT} = \int_0^t \int_q \varepsilon(\lambda) C(q,t) \varphi(\lambda, q, t) dt dq \qquad \textit{Equation 2-4}$$

where

ε : extinction coefficient of the photosensitizer

C : photosensitizer concentration
φ : fluence rate
q : generalized spatial coordinate
t : treatment time

This equation is theoretical and is hard to calculate in practical applications due to unknown extinction coefficient (ε) and concentration (C) of the photosensitizer[2].

In practical applications the total dose is calculated by multiplying the fluence rate in the tissue and the treatment time. Doses between 30 and 540 J/cm^2 has been tested and in Lund the most commonly used dose is 60 J/cm^2 for superficial tumors[13].

Although there are some complications with the dose planning in PDT the planning is motivated by the increased treatment selectivity compared to other techniques where ionizing radiation is used.

2.5.4. Interstitial photodynamic therapy

With the development of optical fibers remote tumors inside the body can be reached through, for example, endoscopes[1]. The light is then guided through the optical fibers directly into the tumor and with the correct dose planning only the tumor is subject to a lethal light dose. This increases the selectivity even more while it gives the physician an alternative to treat solid tumors inside the body. Positive clinical results have been achieved after treatment of liver lesions with optical fibers as well as light emitting diodes placed inside the liver[1].

In Lund an interstitial photodynamic treatment system has been developed which is described in the following chapter.

3. Interstitial photodynamic therapy system

This chapter deals with the IPDT system developed at the Atomic Physics Division at Lund University and SpectraCure AB, Sweden. The system not only carries out a treatment using optical fibers to deliver laser light, but repeatedly measures the light in the tumor, enabling interactive dosimetry as the treatment session progresses.

The system is aimed to be used after administration of ALA to the patient[14].

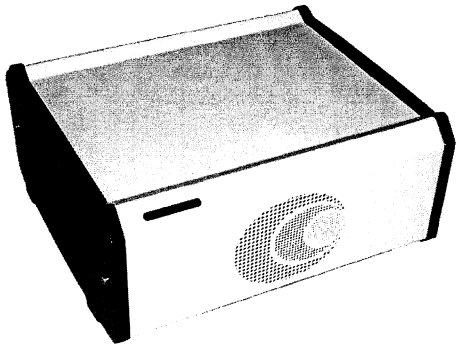

Figure 3-1. IPDT system developed at Atomic Physics Division, Lund Institute of Technology, and SpectraCure AB, Lund. Courtesy of SpectraCure AB.

3.1. Treatment session

This section describes how a treatment procedure is conducted using the IPDT system.

3.1.1. Preparation

When beginning a treatment the first thing to do is to make a 3D-image of the tumor using ultrasound, CT-scan, MRI or the trained hands and eyes of an oncologist. The 3D-image is inserted into a computer dosimetry program which calculates optimal fiber positions, light power and treatment time, based on tissue properties, both for the tumor and surrounding sensitive tissue.

The next step is insertion of optical fibers into the patient's tumor. It is difficult to place the fibers in the optimal positions given by the dosimetry program, due to the elasticity of internal human organs. By using ultrasound imaging during insertion it is possible to see the fibers make their way into the tumor. Hopefully, it will be possible to place the fibers with millimeter precision.

When the fibers are in place, a final imaging of the tumor should be made, where the actual fiber coordinates can be extracted. The dosimetry program is run again, now using the real fiber coordinates, giving new values for light power and treatment time.

3.1.2. Treatment

The IPDT system repeatedly alternates between two modes, Treatment and Diagnostic, during a treatment session. In Treatment Mode all fibers emit light for the photosensitizer to absorb and treat the tumor. Treatment Mode is run for 30-120 seconds, at which time it is interrupted for Diagnostic Mode (Figure 3-2). This lasts for 45 seconds, in which light transmission, photosensitizer concentration and tissue oxygenation are monitored by letting each fiber emit diagnostic light to be detected by the others. This allows for adjustment of laser power and treatment time to better fit the light transmission properties of the tumor. Treatment Mode is then resumed.

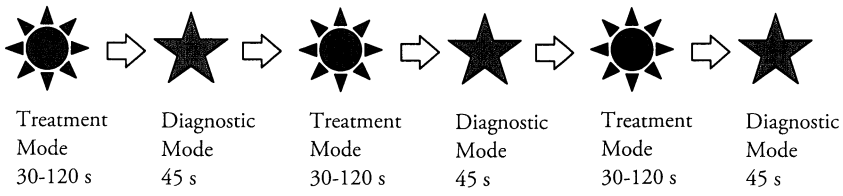

Figure 3-2. Treatment session outline[15].

3.2. *System outline*

A schematic picture of the IPDT system is seen in Figure 3-3.

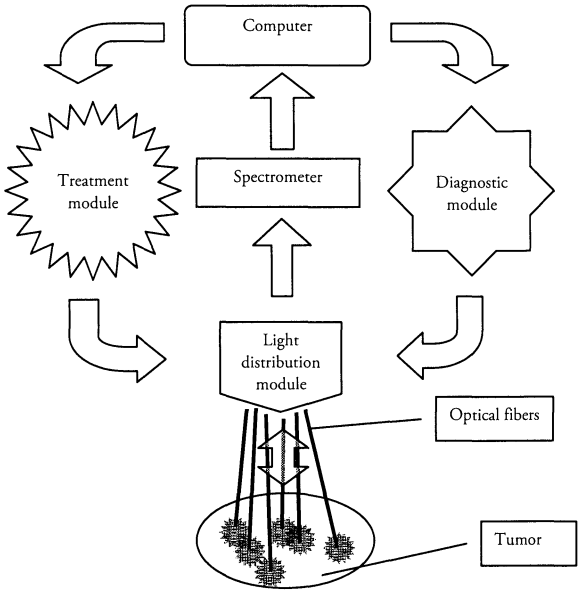

Figure 3-3. IPDT system outline[14].

3.2.1. Laser diodes

The most important property for the IPDT-system is its ability to deliver laser light to the tumor. Laser diodes are used as light sources. The laser light is monochromatic which means that most of the power is emitted in a narrow wavelength region. The laser has a wavelength of 635 nm with a spectral width of ± 1 nm, according to the manufacturer (High Power Devices Inc.).

The laser light is produced when a semiconductor material is subject to a voltage. This induces laser action and light is sent out with the wavelength corresponding to the band-gap of the laser diode[6].

The voltage is controlled by a laser driver, directed by a Control signal (Ctrl) from the software. A total of seven laser diodes are used; six for delivering the therapeutic light and the seventh for performing one of the diagnostic measurements.

3.2.2. Fiber coupled light divider

The treatment is done by placing a certain number of optical fibers inside the tumor. To be able to both deliver and collect light through these fibers Svanberg et al. have developed a light divider that manages this issue[16], called "Rotunda".

Two round metallic discs are placed close together. One of these discs is fixed while the other is able to rotate. On the fixed disc twelve

optical fibers are connected with SMA-connectors. Six of these come from the laser diodes used to deliver light into the tissue (treatment lasers). One is connected to a fiber coupler, described below, and the other five are coupled into a spectrometer.

On the movable disc only six fibers are connected. These fibers are the ones that are inserted in the patient (Figure 3-4).

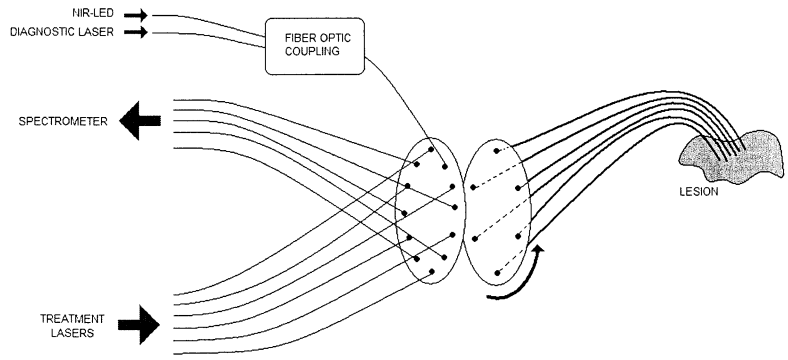

Figure 3-4. Rotunda fiber couplings [15].

The fiber coupler lets the user choose which light source to use during diagnostic measurements. The light source can be a laser of the same kind as the treatment lasers or a near infrared LED. These are explained in section 3.3.2.

The fiber couplings between the rotunda discs induce transmission losses, which have to be calibrated for.

3.2.3. Optical fibers

When light is transmitted through optical fibers the power will be attenuated. The light is guided based on internal reflection. The acceptance angle (α) of the incident light is defined by the refractive indices of the core (n_{core}) and the cladding ($n_{cladding}$), see Figure 3-5. This relation is often characterized by the numerical aperture (NA). Following equation holds[17]:

$$NA = n_{media} \sin\alpha = \left(n_{core}^2 - n_{cladding}^2\right) \qquad \textit{Equation 3-1}$$

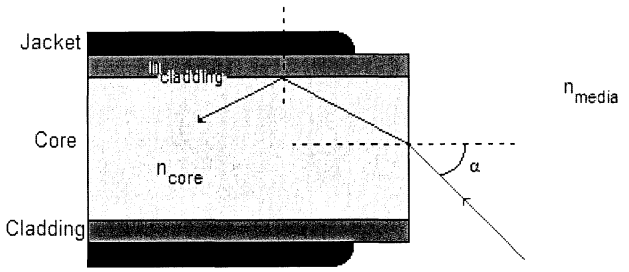

Figure 3-5. Light transport through optical fiber[17].

Due to the numerical aperture the light will be emitted in a cone shaped light distribution with the top angle 2α. Likewise only light incident within this cone can be collected by the fiber, see Figure 3-6.

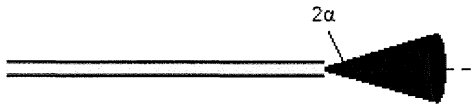

Figure 3-6. Light acceptance cone of optical fiber[18].

Depending on what wavelength-interval should be transmitted the materials can vary. Often used is silica core with doped silica cladding or plastic core with silicone cladding. Power is dissipated in every reflection against the cladding hence the length of the fiber is a large contributor to the losses.

3.3. Therapeutics with the IPDT system

The system utilizes two modes; Treatment Mode and Diagnostic Mode. In Treatment Mode the six treatment lasers deliver light to the lesion. In Diagnostic Mode one of the two light sources mentioned in section 3.2.2 delivers light into the tissue via one fiber while the other five fibers collect light propagating throughout the tumor. The wavelength and the amount of photons collected by the fibers are measured by the spectrometer.

The rotunda is used to switch between Treatment and Diagnostic Mode. As the movable disc turns, new fiber combinations are made. A turn of 30 degrees switches between the two modes[15].

3.3.1. Treatment Mode

During Treatment Mode all six fibers emit light into the tumor for the light sensitizer substance to absorb. The treatment takes place during 30-120 seconds, at which point it is interrupted for the Diagnostic Mode (45 seconds) and then resumed[14].

The rotunda positioned in Treatment Mode is seen in Figure 3-7.

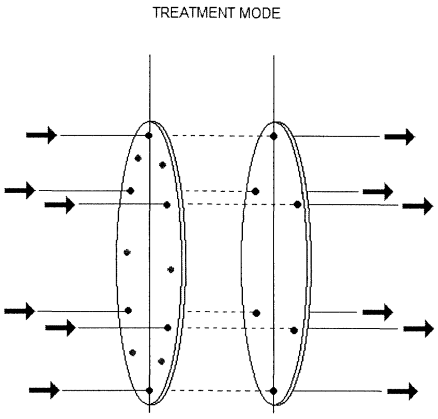

Figure 3-7. Rotunda position in Treatment Mode[15].

A turn of 60 degrees alternates between treatment lasers for the fibers inserted into patient.

3.3.2. Diagnostic Mode

During Diagnostic Mode one fiber emits light and the other fibers detect the transmitted light inside the tissue. To position the rotunda in Diagnostic Mode the movable disc rotates 30 degrees from the Treatment Mode position. A fiber coupling device switches light source between laser (635 nm) and near infrared LED. The light collected by the five fibers is led to a spectrometer where the spectral composition and intensities are registered in five channels. This is a way to monitor the light transmission inside the tissue during the treatment session. After one fiber has emitted light the rotunda rotates 60 degrees to let another fiber emit the diagnostic laser light and the others detect it[15]. Figure 3-8 shows the rotunda positioned in Diagnostic Mode.

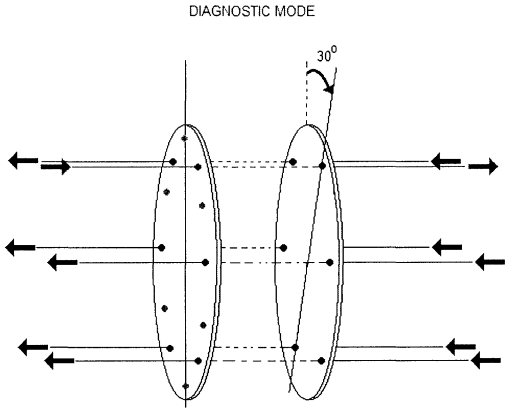

Figure 3-8. Rotunda position in Diagnostic Mode[15].

3.3.2.1. Fluence rate

The main thing to measure is the light fluence rate. This dictates how much light is propagating inside the tissue. The light source used is the diagnostic laser. When measuring the light, only a certain part of it will really enter the fiber to be detected, due to the light acceptance cone of the optical fiber. This is however not a problem if only relative values are wanted.

The detected light seems to diminish during the treatment, perhaps due to increased blood content in the tissue as small blood vessels in the tumor break[14]. This online monitoring of the light fluence rate makes it possible to alter the dosimetry calculations during the treatment, e.g. increasing the laser power from certain fibers or prolonging the treatment time to compensate for the decreased light transmittance.

3.3.2.2. Photosensitizer concentration

As the treatment progresses photobleaching occurs, in which the photosensitizer drug is consumed. To monitor the amount of photosensitizer left in the tissue, fluorescence specific for the drug is studied. This is achieved by using the diagnostic laser as a light source. ALA fluoresces at a NIR wavelength, 705 nm, when excited by the ordinary 635 nm laser[14].

3.3.2.3. Oxygen saturation level

Oxygen is needed for the PDT treatment. Deoxy-hemoglobin and oxy-hemoglobin are two similar molecules, differing in that deoxy-hemoglobin carries no oxygen but oxy-hemoglobin does. Deoxy-hemoglobin is a much stronger absorber of light with wavelengths below 800 nm than oxy-hemoglobin, but they absorb equally much at 800 nm (Figure 3-9). By using the NIR-LED as light source to compare absorbance ratios between the two molecules at approximately 800 and 760 nm, the oxygen saturation level (S_{O_2}) can be calculated and monitored throughout the treatment using Equation 3-2 [14].

$$S_{O_2} = \frac{[HbO_2]}{[Hb]+[HbO_2]} \qquad \textit{Equation 3-2}$$

As oxygen is consumed during PDT, the ratio of deoxy-hemoglobin relative oxy-hemoglobin will increase.

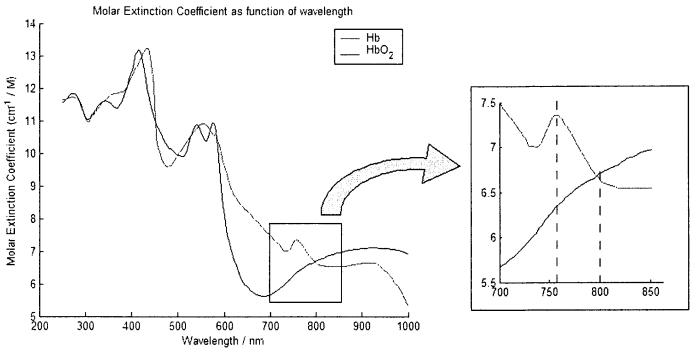

Figure 3-9. Absorption coefficient for deoxy- and oxy-hemoglobin [19].

3.4. *System losses and the need for calibration*

The diode lasers in the IPDT system age and their maximum output power decreases with time, making the same drive current give a lower emitted power. This is one of the reasons stating the need for a calibration of the emitted laser power before each treatment session.

There are no fiber couplings with zero loss in light transmission. Since new sets of sterile fibers are to be used in each IPDT session, the coupling losses are different from one treatment session to the next. The fibers themselves also differ in transmittance, especially if the bare fiber end has not been polished enough or has been damaged during assembly or transport. Laser power output as well as measuring capability are thereby compromised and need calibrating.

The two important aspects of the spectrometer is its overall sensitivity to light and its ability to divide up the light spectrally. The spectral calibration was not a part of this Master's Thesis project.

3.5. *Fiber holder*

The patient fibers, see Figure 3-10, are inserted into the patient and are supposed to be sterile. New patient fibers are to be used for every treatment and will be delivered in a package. The calibration procedure should be a simple maneuver. It should be possible to just take out the fiber device from the sterile package, attach one end to the IPDT system and the other to the Calibration unit.

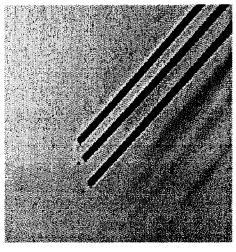

Figure 3-10. Bare-end optical fibers.

4. Calibration alternatives

Two properties of the IPDT system have to be calibrated for; emitted laser power (Treatment Mode) and its light fluence rate measurement capability (Diagnostic Mode). This chapter presents the alternatives that have been considered and evaluated; two alternatives for Treatment Mode and four alternatives for Diagnostic Mode calibration.

4.1. Treatment Mode

The calibration for the Treatment Mode is rather straightforward: measure the light exiting the optical fibers and correlate this with the drive signal that controls the laser diodes. A higher drive value to a laser diode may be needed at one treatment session compared to another to achieve an equal fiber output power.

The powers used during treatment are in the interval 20 -150 mW. The calibration should therefore be done for three to five different values in this interval to achieve a linear calibration graph. The calibration graph for each fiber should look like:

$$P = k \cdot C + m \qquad \textit{Equation 4-1}$$

where:

P:	Light power emitted from fiber (mW)
C:	Control signal to laser driver (counts)
k, m:	Linear coefficients

4.1.1. Integrating sphere

The first alternative considered was the integrating sphere, which would combine the Treatment and Diagnostic Mode calibrations into a single device.

4.1.1.1. What is an integrating sphere?

An integrating sphere receives light through a port on the sphere perimeter, see Figure 4-1. The inside coating is made of a highly reflective material (e.g. Spectralon® or barium sulfate, $BaSO_4$). The incoming light is reflected several times on the inner surface and a

uniform diffuse irradiance across the sphere's area is generated. A photodiode is placed on the inner wall to measure the light power. The ratio between the photodiode's area and the sphere's inner area is important. If the photodiode's area is 1/1000 of the sphere's area, the photodiode only measures a 1/1000 of the total light. The total power exiting the fiber is calculated by dividing the measured power with the area ratio (<1).

Figure 4-1. Oriel integrating sphere.

The detected light is influenced by the reflectivity of the inside coating (typically 98%) and the total area of the input and output ports. No reflection occurs at the ports, which means that the irradiance does not become really uniform. A rule of thumb is to keep the ports' area below five percent of the total area to achieve an irradiance that is adequately uniform[20].

4.1.1.2. General idea

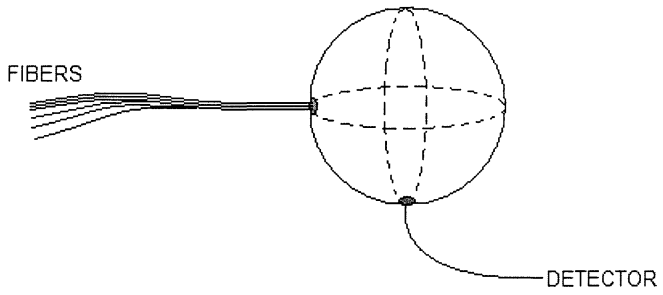

Figure 4-2. Integrating sphere (Treatment Mode calibration).

The fibers are kept in a bundle. The bundle is attached to the sphere's input port and one by one the fibers emit light for calibration. The light is diffusely scattered inside the sphere and the irradiance on the

inner surface becomes uniform. A photodiode on the inside perimeter detects the light power and gives an electrical current.

4.1.1.3. Problems

An integrating sphere is expensive, 10000-40000 SEK, which is an important aspect since it would be a component of the calibration unit, which itself is a component of the larger IPDT system.

The sterility guidelines for medical equipment must be fulfilled. The integrating sphere might be used with some shielding that can be disinfected to protect the sterile fibers.

4.1.2. Photodiode

4.1.2.1. What is a photodiode?

A photodiode is a light sensitive device made of a semiconductor material that generates an electrical current when hit by electromagnetic radiation (light) with the right energy (wavelength).

4.1.2.2. General idea

The simplest way to measure the light exiting the fibers is to let the fibers illuminate a photodiode and measure the generated current, see Figure 4-3. A problem to be wary of is making the entire cone of light fit onto the photodiode's sensitive area. Therefore the fibers should be placed tightly in a bundle, as seen in Figure 4-3.

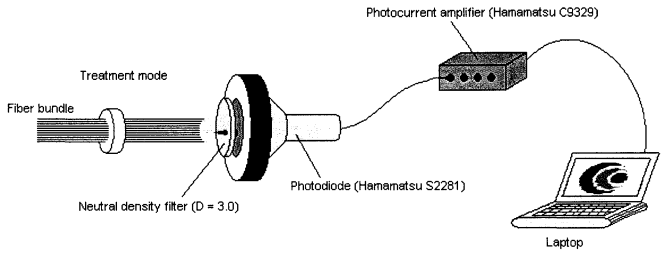

Figure 4-3. Treatment Mode measurement using a photodiode.

The light from each fiber in the bundle hits a large area photodiode (Hamamatsu S2281). The current from the photodiode is proportional to the incident light level and is converted into digital signals by the amplifier (Hamamatsu C9329).

4.1.2.3. Measurements

Tests were conducted to get qualitative information about the photodiode alternative.

First, the influence on the power measurements by the emitting fiber's distance to the detector was investigated. The fiber, emitting HeNe-laser light, was pulled back from its initial position (2 mm from detector head). The power meter (Ophir) monitored the declining power as a function of distance. Within a few millimeters the power only decreased 1% relative the initial position's power reading. The goal is to keep the illuminated area on the photodiode as small as possible, without saturating the photodiode. The fiber bundle must be as close as possible to the photodiode, ensuring that each fiber's light cone fits onto the diode.

Secondly, the emitting fiber was placed in a fiber bundle consisting of 18 fibers. To test how much the adjacent fibers attenuate the delivered light the emitting fiber was pulled back into the bundle. In the initial position all fiber tips were aligned. Only when the fiber was pulled back behind its neighbors' jackets did the power drop down to 98% relative the initial position's power reading.

4.1.2.4. Problems

The photodiodes investigated were made of silicon. According to the manufacturer these photodiodes had linear response up to 10^4 lux which is approximately 6.7 mW on the entire detector area. To keep the incident light level below this limit an attenuating ND-filter (neutral density) is needed. This would reduce the light with a factor of 10^2-10^4, depending on which filter would be used. The filter and the photodiode need to be calibrated together as one system during construction in order to relate detected power to the measured current.

If the laser beam spot is too small the irradiance could exceed the limit for linearity and damage the photodiode.

All light from the fibers should fit onto the photodiode, otherwise some light is lost and the drive signals for the laser diodes are increased to compensate for what the system interprets as a transmission loss in the fibers. Since a photodiode is also less sensitive to light at its edges, the light from the fibers should hit the center of the photodiode.

4.2. Diagnostic Mode

The calibration of the Diagnostic Mode is more complicated than the Treatment Mode calibration. Ideally, all fibers would collect an equal amount of photons and the detecting spectrometer at the other end of the fibers would measure each fiber path's resulting light intensities after propagation through the system (Figure 4-4).

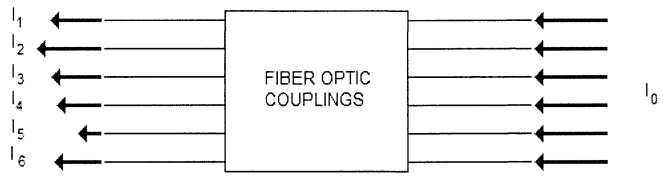

Figure 4-4. Schematic picture of the Diagnostic Mode light paths.

Preferably the incoming light irradiance (I_0) should be known. The absolute calibration is then done by relating each fiber response (I_1 – I_6) to the incoming (I_0). This is made for three to five different incident powers. The number of counts on the spectrometer is then related to the light power by a calibration graph, such as:

$$I_i = k_i \cdot c + m_i \qquad \textit{Equation 4-2}$$

where:

I : Light power detected by the spectrometer (mW)

c: Number of counts detected by the spectrometer (counts)

k_i, m_i: Linear coefficients for fiber i.

Another way to calibrate the system is by relative calibration. The incoming light irradiance (I_0) is equal for all fibers but it is not known. By relating the fiber responses (I_1-I_6) to one fiber (e.g. I_1) each fiber path's losses can be calculated relative to this fiber.

$$\frac{I_i}{I_j} = k_{ij} \quad k_{ij} = 1, if\ i = j \qquad \textit{Equation 4-3}$$

where:

I_i, I_j: Light detected by the spectrometer (counts)

k_{ij}: Relative loss for fiber i related to fiber j.

The IPDT system would use the calibration set with fiber path losses to adjust its Diagnostic Mode measurements.

4.2.1. Detected power interval

The calibration should be done in the same power interval as during the treatment session. Since this kind of calibration never has been done on the system the typical detected powers were unknown. Therefore some simple light diffusion simulations were performed.

The fluence rate as a function of distance from the light source was calculated with Equation 2-1 for different incident light levels (30-150 mW). The power was calculated from the fluence rate according to Equation 4-4[20]. The radiometric definitions are shown in Appendix A.

$$P_{fiber}(r) = L \cdot A_{fiber} \cdot \Omega_{fiber} \qquad \textit{Equation 4-4}$$

where:

P_{fiber}: power detected by fiber (W)

L : radiance (W/m^{2}sr)

$\Omega_{fiber} \approx \pi NA^2$: solid angle for light acceptance cone of fiber (rad)

$A_{fiber} = \pi \cdot r_{fiber}^2$: Area of the fiber-tip (m^2)

Using Equation A-1, Appendix A, for an isotropic light distribution, i.e. the radiance is constant, Equation 4-4 becomes:

$$P_{fiber}(r) = \frac{\phi(r)}{4\pi} \cdot A_{fiber} \cdot \Omega_{fiber} \qquad \textit{Equation 4-5}$$

The calculated powers can be seen in Figure 4-5. The tissue optical properties used were $\mu_s' = 12.0$ cm^{-1}, $\mu_a = 0.16\,\text{cm}^{-1}$ for normal tissue and $\mu_s' = 12.4$ cm^{-1}, $\mu_a = 0.31\,\text{cm}^{-1}$ for tumor tissue[14].

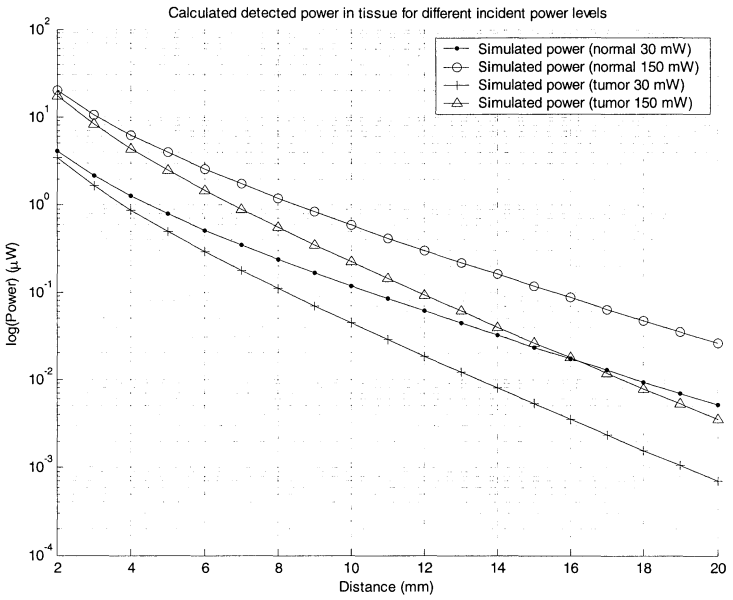

Figure 4-5. Simulated detected power in tissue detected with 400 micrometer diameter optical fiber.

Although the approximations made are quite rough we concluded that the power interval for the detected light is between 10 nW-10 μW.

4.2.2. Tissue phantom

The spectrometer's detected intensity is calibrated against what the diffusion approximation predicts the light fluence rate to be at the fiber tips in a homogenous, scattering medium.

4.2.2.1. What is a tissue phantom?

To simulate organic tissue, a tissue phantom may be used. This phantom can be made to have the same scattering and absorbing properties as tissue. In the study of how light is transported through

tissue, phantoms are widely used. Intralipid®, a milky white fatty substance, mainly used for intravenous feeding, is a popular phantom. The fat particles, lipids, scatter light. By diluting Intralipid® with distilled water, the solution's concentration is altered and with it the scattering property. An Intralipid® solution with high concentration has high scattering, a low concentration has low scattering.

To control the absorption, ink is usually added to the solution. The more absorber substance added to the solution, the higher absorption coefficient.

4.2.2.2. General idea

The goal is to have a known fluence rate at the fiber tips and correlate this to the spectrometer's detected values. One fiber delivers the light and the others detect it, seen in Figure 4-6. The detected signals on the spectrometer are related to a solution of the diffusion approximation for the distances between the source fiber and the detector fibers. A Diagnostic Mode calibration would thereby be achieved. By keeping the fibers at precise positions relative each other, the fluence rate at the fiber tips could be predicted more easily.

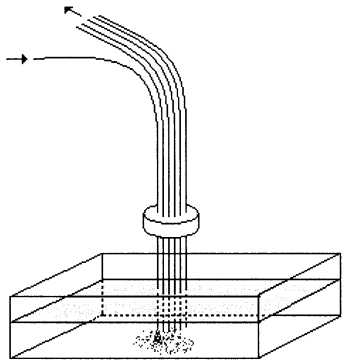

Figure 4-6. Measurement calibration using an optical phantom and the diffusion approximation.

The calibration phantom would probably be delivered in a small hard plastic cup with a thin plastic film on top for the fibers to penetrate. Probably no more than a deciliter phantom would have to be used. This is an absolute calibration alternative.

4.2.2.3. Problems

The fluence rates at the fiber tips are not measured directly but calculated theoretically, which is a major source of error. We would want to know how much light enters a fiber at a certain location in the phantom, but here we only assume that the entering light equals what the diffusion approximation predicts. Boundary effects due to the cup's walls are a problem for the diffusion approximation. This

could be eliminated by using a large cup, but practical product considerations have to be taken into account. The fibers themselves will affect the light distribution in the phantom. The black plastic fiber jacket absorbs light and shields the other fibers from the light, which seriously throws off the diffusion approximation.

The fibers are to be sterile when used in the treatment and avoiding contamination is a must. Dipping the fibers into the Intralipid® phantom would let residue assemble on the fibers, which perhaps could be washed off with alcohol, but still constitutes a problem.

The phantom should be easy to reproduce to get the same optical properties in every calibration phantom unit. If the properties are not well-defined, the diffusion approximation would predict false fluence rates and the calibration would be faulty. Unfortunately Intralipid® phantoms are hard to reproduce with the same optical properties[21]. The phantom may also lose their defined optical properties as they age over only a couple of months. The risk of users storing calibration phantoms past their expiring date seems high.

4.2.3. Integrating sphere

The integrating sphere would combine the Treatment and Diagnostic Mode calibration in one device.

4.2.3.1. General idea

The fiber bundle is attached to one of the sphere's ports, see Figure 4-7. An external light source delivers light into the sphere. A uniform irradiance is created inside the sphere and all fibers in the bundle are hit by the same amount of light.

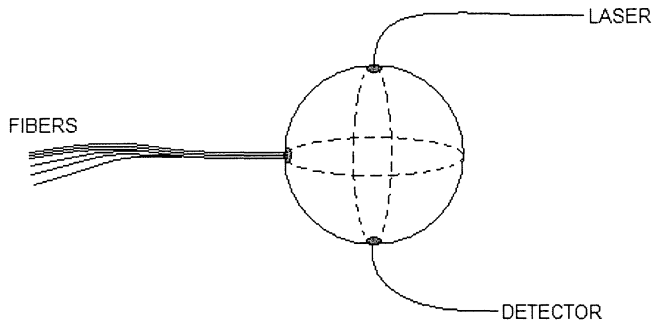

Figure 4-7. Integrating sphere (Diagnostic Mode calibration).

The photodiode measures the diffuse light irradiance, just as in the Treatment Mode calibration (4.1.1.2), to control that the external light source transmits the desired light power.

To achieve an even light distribution within the sphere, the detector (the fibers) can not be located where the light source (emitting fiber) is because the fibers would register a first reflection from the far wall, and not the uniform irradiance. The light entering the sphere has to bounce around before it becomes diffuse. The light source should therefore be located 90 degrees from the detector. The external light source could be a diode laser, same type as in the IPDT system itself, or an LED, assuming that the wavelength is correct and the output light power interval can be reached.

This is an absolute calibration alternative.

4.2.3.2. Problems

The problems are the same as for the Treatment Mode calibration, discussed in section 4.1.1.3. The shielding, used to keep the fiber bundle sterile, would unfortunately affect the light distribution thus making it hard to achieve a uniform light distribution at the fiber tips. Also, there may not be sufficient light power when using an LED as external light source. Electronics to drive and control the external light source from within the IPDT system program would also be needed.

To make sure the fibers receive the same light irradiance at their tips they must all be aligned with the inner wall. With the fibers kept in a bundle this could be a problem. A sophisticated holder or coupling mechanism attached to the sphere's input port would be required. Modifying a commercial integrating sphere to accommodate a custom-built fiber bundle holder was deemed too complicated for this project.

4.2.4. Diffuse transmittance

A uniform light field is generated using an array of light emitting diodes (LEDs) and a glass diffuser plate.

4.2.4.1. General idea

An LED array is placed under a diffusing ground glass plate, according to Figure 4-8. The glass plate creates a uniform irradiance over a reasonably large area. Optimally, all fibers will receive equal light power in the region 10 nW -10 µW. The drive signal to the LED-array should be controllable so that a few predetermined light powers can be emitted. To control in what power interval the fibers are detecting a small photodiode is placed close to the fibers. The fibers can then be calibrated against the photodiode standard.

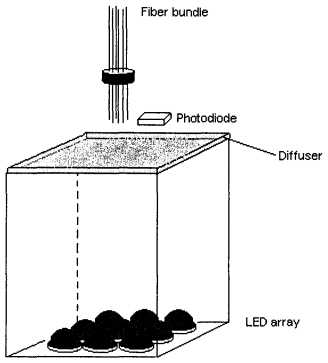

Figure 4-8. Diffuse transmission using an array of light emitting diodes.

The distance between the diffuser and fibers should be chosen so that the power is in the correct interval and the irradiance is uniform.

This is an absolute calibration alternative provided that the photodiode is used. Otherwise the method is only relative since the power reaching the fiber tips would be unknown.

4.2.4.2. Measurements

The first test made with the LEDs consisted of translating a fiber, coupled to a power meter, in two dimensions above the LED array (Figure 4-9a) at a distance of where the fiber bundle would be located. To make the uniform area large enough for all fibers to be inside it, plates of different material were tried out as diffusers. Plastic materials, such as Delrin (Figure 4-9b), and ground glass diffusers from Thorlabs, USA, were tested. The diffusers differed in transmittance and diffusivity.

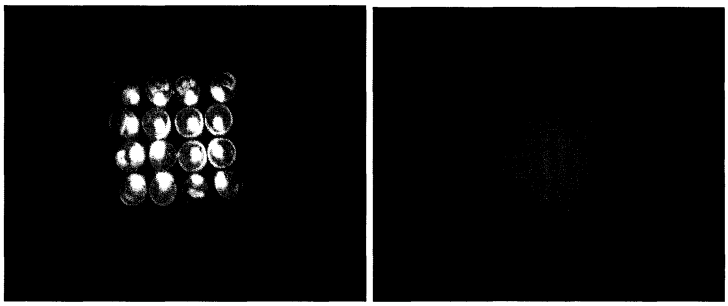

Figure 4-9. a) Array of sixteen Toshiba LEDs b) Transmitted diffuse light field on top of Delrin diffuser.

The power readings were registered and analyzed in Matlab. A map of the translated area showing the light irradiance at each measuring point was generated (Figure 4-10).

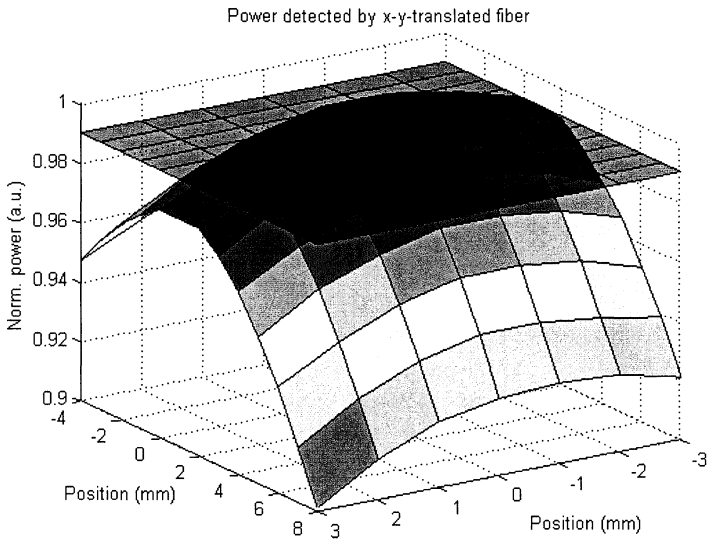

Figure 4-10. Irradiance map by fiber translation of LED array. Blue plane indicates a reduction of one percent from the top value.

In Figure 4-10, a reduction of maximum one percent from the top value is reached within an area of 4x4 mm.

4.2.4.3. Problems

To drive and control the LED array a set of electronics is needed. The electronics should be connected into the IPDT system and controlled by the main operating program.

The second problem is that the lasers, in the IPDT-system, are spectrally narrow (FWHM about 1.5 nm) while the LEDs are broad (see Figure 4-11). The peak wavelengths also differ, although the LEDs and the lasers are both red to the human eye. In front of the spectrometer inside the IPDT system is a wavelength-dependent filter, designed to suppress the 635 nm laser treatment light to allow for longer exposure times for the fluorescence measurements at longer wavelengths (NIR).

If the calibration light source is not the same as what the IPDT system will detect in Diagnostic Mode during a treatment, the detected signal will be biased according to the LEDs own spectral emission map, the wavelength filter's sensitivity curve and the spectrometer's own spectral sensitivity, which is not uniform. As the laser diodes and the LEDs heat up during use their respective peak wavelengths will drift, making the problem even worse.

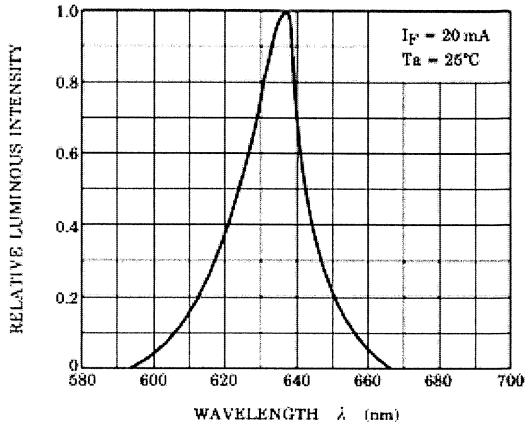

Figure 4-11. Spectral emission chart for Toshiba TLRMH156P LED. LEDs are spectrally broader than laser diodes. Here the spectral width at half maximum is 20 nm[22].

The third problem is to achieve a large enough area of uniform irradiance in front of the fiber bundle. Depending on how large this area is, the chance of one fiber in the bundle falling just outside the uniformity area changes.

4.2.5. Diffuse reflectance

Because of the wavelength-dependent filter in front of the spectrometer a different version of the diffuse transmission was developed. In the diffuse reflectance alternative the IPDT system's own laser light is used to create a uniform irradiance.

4.2.5.1. General idea

A laser beam does not have a uniform intensity distribution over its cross-section. The spot profile has a Gaussian distribution, as seen in Figure 4-12.

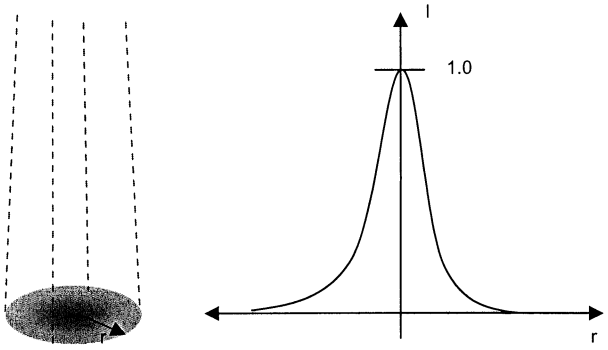

Figure 4-12. A projected laser beam spot with radius r. The light has a higher intensity in the center, due to its Gaussian intensity distribution profile[23].

The diffuse reflectance alternative features the fibers positioned in a bundle, where one fiber delivers light from the diagnostic laser diode. The light passes a diffusing plate and is reflected by a mirror, again passing the diffuser on the way back (Figure 4-13). The light field closest to the emitting fiber is now diffuse, which means the irradiance variations seen in Figure 4-12 are evened out. To a first approximation all fibers in the bundle thereby receive the same amount of photons.

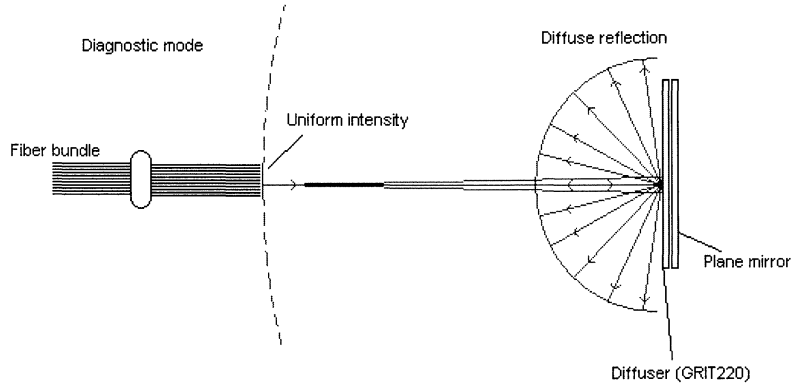

Figure 4-13. Uniform light field after passing the diffuser and beeing reflected.

The distance from the fiber bundle to the reflector unit is of great importance. The longer the light has to travel, the more divergent it becomes, which means the area with uniform irradiance grows[23].

In a bundle of six fibers, the maximum distance from one fiber to another is two fiber diameters (see Figure 4-14). Hence equal irradiance within at least a radius of two fiber diameters from the emitting fiber should be achieved.

Figure 4-14. Bundle of six fibers. One fiber emitting laser light.

If the bundle contains eighteen fibers, there would be a need for equal irradiance within a radius of four fiber diameters (3.2 mm).

The diagnostic fiber emits light at a few predetermined power values, which should yield calibration points in the interval 10 nW to 10 µW, which is what will be detected when measuring the power transmitted inside the tissue during a treatment session. The neighboring fibers are collecting the reflected light (Figure 4-15a).

Since the fibers are placed tight in a bundle the detecting fibers will not only collect the diffusely reflected light, but also the light leaked from the emitting fiber, see Figure 4-15b.

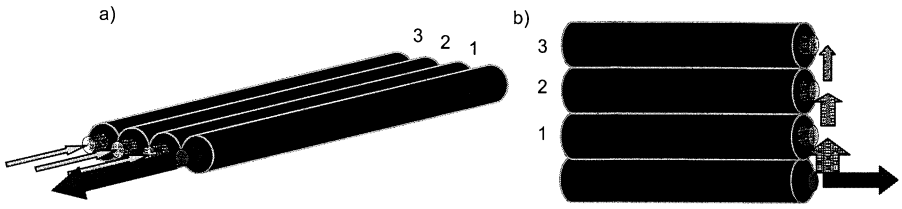

Figure 4-15. a) Diffuse reflectance. One fiber emits, the others collect. b) Light leakage from emitting fiber to neighbors. The numbers are used to indicate the fiber positions.

To compensate for this leakage a reflector blocker has to be used. By subtracting the reflector blocker measurements from the diffuse reflector measurements, the leakage is compensated for. The reflector blocker should have low reflectance, optimally none, and the reflected irradiance should be uniform. With a uniform reflectance all fibers would receive an equal offset in detected light.

This is a relative calibration alternative.

4.2.5.2. Measurements

The aim of these measurements was to investigate the area where the diffusely reflected light has uniform irradiance.

The tests were confined to a cardboard box (Figure 4-16). The reflector unit was constructed with a ground glass plate (GRIT 220, Thorlabs) combined with a plane mirror. This was placed at distances ranging from four to sixteen centimeters from the fiber bundle.

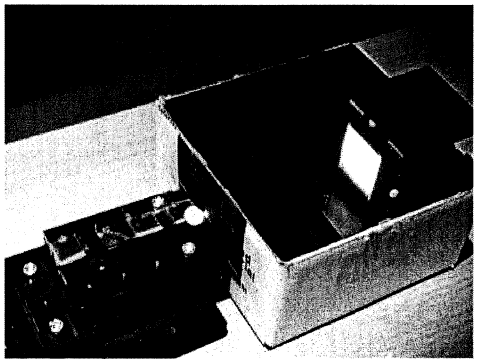

Figure 4-16. Measurement setup during diffuse reflectance measurements. Laser light hits the reflector unit and returns back to the fiber bundle. Reflector blocker (black paper square) lies on top of the reflector unit.

The emitting fiber was positioned according to Figure 4-15 while the detecting fiber was altering placed at position 1-3. Extra fibers were placed between emitting and detecting fibers to mimic the condition in the fiber bundle.

The diffuse reflectance was measured for three different light powers (10 mW, 33 mW and 70 mW). The reflectance from the

reflector blocker was measured by placing a paper plate in front of the reflector unit (Figure 4-16). The results for the 12 cm distance between reflector unit and fiber bundle are shown in Figure 4-17.

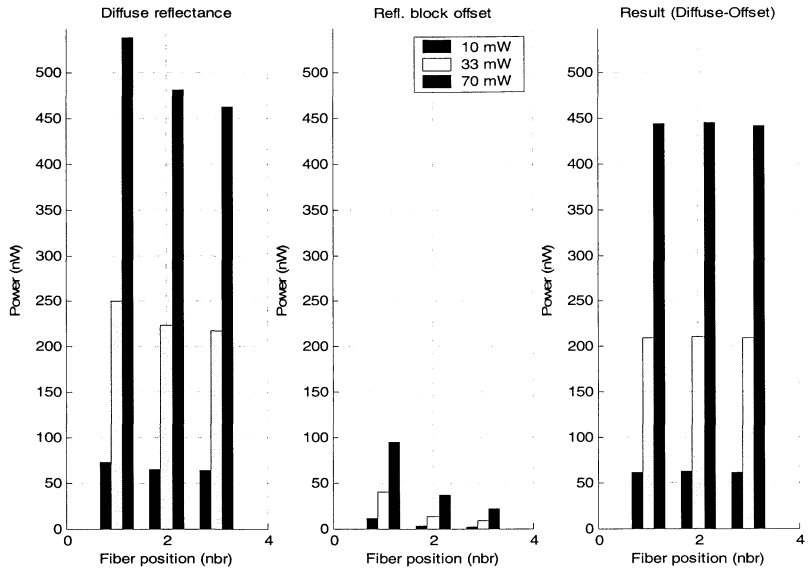

Figure 4-17. Detected power for different fiber positions.

The deviation of the compensated results is approximately 0.5%, relative position 1, for all three powers. The best uniformity in the irradiance was achieved in the range of ten to fourteen cm between reflector unit and fiber bundle.

To examine the leakage of light from the emitting fiber to the other fibers, screened measurements were conducted using a thin piece of black paper (Figure 4-18) to screen the emitting fiber.

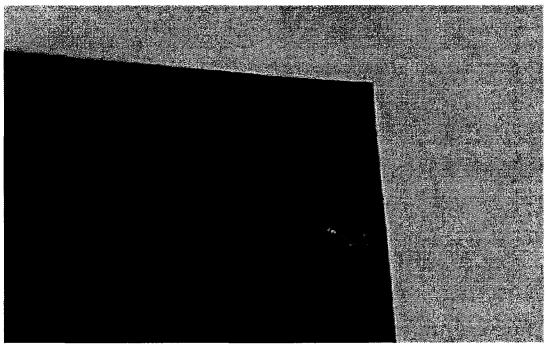

Figure 4-18. Emitting fiber screened off to eliminate light leakage.

The measurements were made in the same way as above, but for the powers 11 mW, 38 mW and 78 mW. The results are shown in Figure 4-19 for distance 12 cm, between reflector unit and fiber bundle.

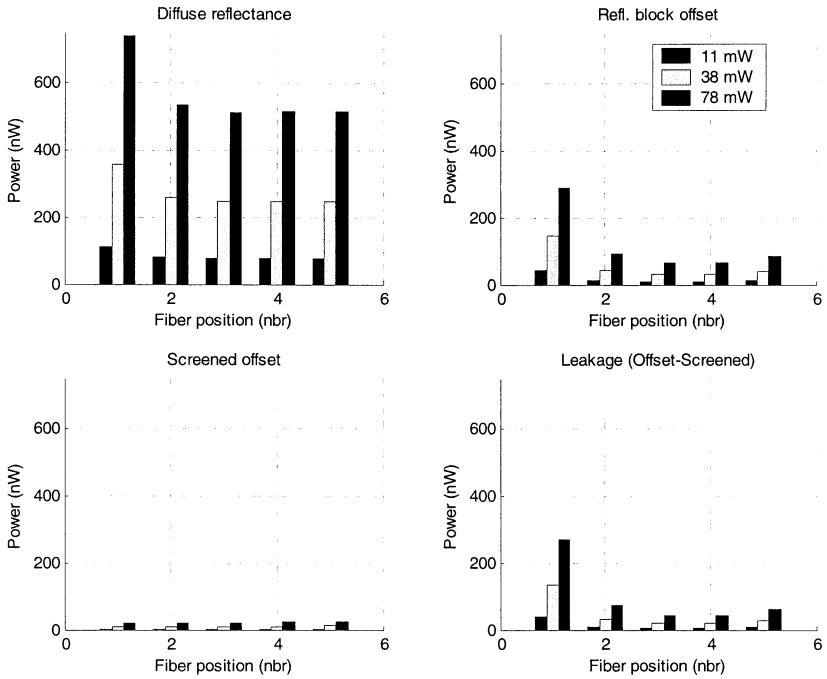

Figure 4-19. Screened offset measurements. Diffuse reflectance measurement is included for comparison.

The screened offset measurement yields an estimate of the reflector blocker's reflectance. As seen in Figure 4-19 the values are small related to the diffuse reflectance. The screened offset is lower than 5% relative the leakage compensated diffuse reflections from the reflector unit. Due to the reasonably low reflectance of the reflector blocker, the leakage compensation can be made as described above.

4.2.5.3. Problems

Achieving a sufficiently uniform reflected light field at the fiber tips could be difficult but the experimental work shows that it is possible. The emitting fiber leaks light over to its neighboring fibers, but this is also examined in the experiments. An absolute calibration of the Diagnostic Mode can not be made since the light irradiance at the fiber tips is not known, only that it is equal over all fibers. A relative calibration among the fibers should be sufficient. Ideally, a photodiode would be positioned right where the fiber bundle is to measure the exact light irradiance, but would then obstruct the fibers.

4.3. Calibration alternative selection

4.3.1. Treatment Mode

It was quickly decided to use some kind of photodiode to measure the laser power. The photodiode is a simple and cheap alternative for measurements of the fiber optic power, as opposed to integrating spheres, which are often used as power meters since they collect all light exiting the optical fiber.

A recent study showed that the uncertainty of the measured power was higher using a plain photodiode than power measurements done with an integrating sphere. The light inside the sphere is diffuse; hence the spatial and angular non-uniformities of the light are negligible. The photodiode is more sensitive to the positioning of the fiber and thereby the uncertainty is increased. Although the study, mentioned above, was performed using longer wavelengths and other photodiodes than in this diploma work, it is evident that photodiodes can be used as a relatively accurate power meter. [24]

A restriction is that the fiber must be placed close to the photodiode so that the entire light cone from the fiber hits the detector area.

4.3.2. Diagnostic Mode

The diffuse reflectance calibration alternative was chosen because of its simplicity. The integrating sphere seemed to be a too expensive alternative to implement and would require complicated modification to accommodate the fiber holder. The tissue phantom alternative was early rejected because of all the problems with the reproducibility of the phantom. The diffuse transmittance alternative seemed to yield good results although this alternative would have been hard to implement with the computer-controlled electronics to control the LEDs. The detected power levels were a bit too low. The risk of fibers falling outside the uniform irradiance area was also high. The diffuse reflectance alternative was therefore the strongest candidate for the implementation. The simplicity of combining the different calibration modes also played a part in the selection.

The implementation is described in the next chapter.

5. Calibration unit implementation

This chapter deals with the work of designing and building a prototype of the Calibration unit after choosing a calibration alternative.

5.1. Prototype construction

Figure 5-1 shows the design of the Calibration unit prototype.

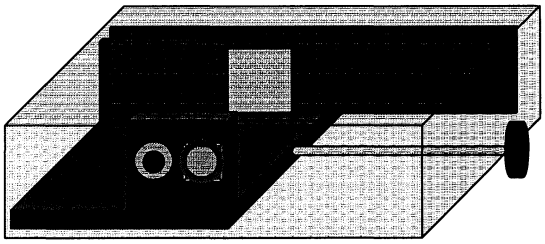

Figure 5-1. Calibration unit.

After the decision of implementing the diffuse reflectance and photodiode version, a way to combine these was figured out. A movable sled carrying components in front of the aperture was designed.

5.1.1. The sled

In our prototype, the sled is translated manually between the four stations by a large screw on the side, but in future versions this would be done by an electric motor.

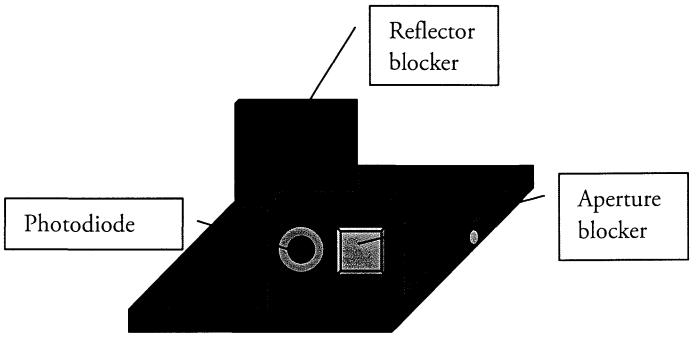

Figure 5-2. Sled design.

When the Calibration unit is not in use, the sled is in Station 1, blocking the aperture to protect against dust entering the unit. Station 2 is Treatment Mode calibration, where the photodiode (Hamamatsu S2281) measures the light power from the fibers. Station 3 is the Offset measurement for the Diagnostic Mode calibration. A black metal plate blocks the reflector unit. Station 4 is the Diffuser measurement, also for Diagnostic Mode. With the black plate out of the way, the light has a non-obstructed path from the fibers to the reflector unit and back.

5.1.1.1. Station 2 (Photodiode)

The light is attenuated by a neutral density filter (optical density 4) with a factor of 10^4 to avoid saturation of the photodiode. The photodiode is connected to an amplifier (Hamamatsu C9329) located outside the calibration unit.

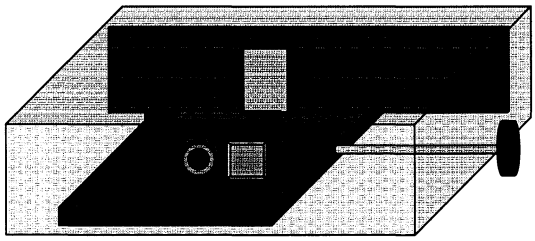

Figure 5-3. Sled in station 2, Photodiode.

5.1.1.2. Station 3 (Offset)

To perform the Offset measurement, the sled is moved to station 3, making the black plate obscure the reflector unit. All fibers emit light from the diagnostic laser diode one by one and reflectance measurement data is taken by the spectrometer.

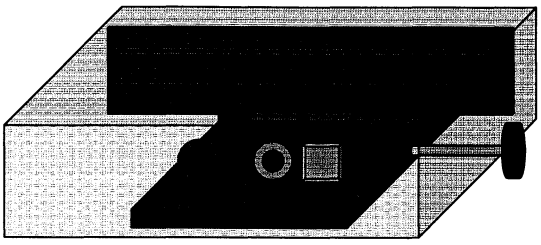

Figure 5-4- Sled in station 3, Offset.

5.1.1.3. Station 4 (Diffuser)

In station 4 the path between the fibers and the reflector unit is free and the diffuse reflectance measurement can be made in the same way as the Offset measurement.

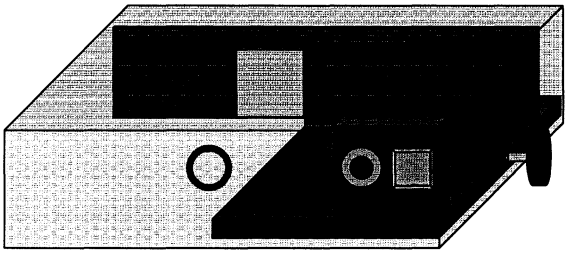

Figure 5-5. Sled in station 4, Diffuser.

5.1.2. Box size

If the box is too small, the light reflected off the walls would probably mess up the irradiance uniformity at the fiber tips. Measurements of diffuse reflectance were carried out in cardboard boxes of diminishing sizes, but no degrading in the uniform light distribution was detected. The size of the prototype is based on the smallest box size tested and calculations of how the fibers' light cones diverge.

The tests of different distances from fiber to reflector unit continued, now concentrated to the ten to fourteen cm range. Several fiber translation measurements were made, as in 4.2.5.2, but none of the distances ten, twelve and fourteen cm could be said to be better than the others. In the prototype unit slits are made in the walls to allow a plate with the reflector unit to be moved between the three distances. This is to allow further tests on the distance to be made on the finished prototype, which is made in aluminum and not cardboard.

5.1.3. Designing the reflector blocker

The purpose of the Offset measurement is to get a reading of the light leakage between the fibers to compensate the Diffuser reading. A complete obliteration of the reflected light during the Offset

measurement is not needed, only a drastic reduction in reflected light to make sure the irradiance is practically uniform.

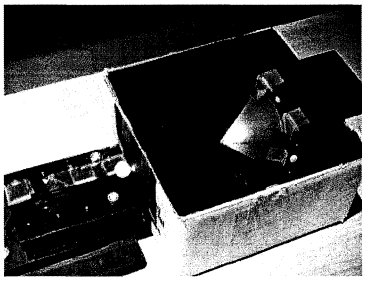

Figure 5-6. Offset measurement using a paper cone as blocker. The plain paper square blocker is seen lying on top of the reflector unit.

In the attempt to minimize the reflected light during the offset measurement, two different reflector blockers were tested. A plain black piece of paper and a black paper cone (Figure 5-6). Our prediction was that the cone would give less reflected light than the paper square since the cone deflects a part of the light to the sides. The collected irradiance was only slightly lower and since a plane square is easier to work with, the piece of paper was chosen.

The fact that the black paper does not give a zero percent reflection is not a problem, since it only gives an offset in the measurement data that is virtually the same for all fiber positions (see Figure 4-19). In the prototype a black anodized metal plate would be used instead of paper, but the principle is the same. Using the cone could also induce a slight problem when the emitting fiber is not exactly in front of the cone. The light would hit the paper cone on the side and not head-on, which could give a skewed reflection.

5.1.4. Fiber holder construction

The fibers will be delivered in a sterile package. The idea is also to have a sterile holder that holds the fibers in fixed positions relative to each other. The holder constructed is thought to be simple. Six fibers are held in a bundle inside a soft plastic tube. A strain relief cord grip clamps the tube and the fibers together. An exterior rigid plastic tube is screwed onto the cord grip to protect the fibers. The end of the exterior tube is threaded so the entire fiber holder can be screwed into place in the Calibration unit. A second cord grip on the other end of the exterior tube helps keep the fibers together. If more than six fibers will be used these could be placed in additional holders.

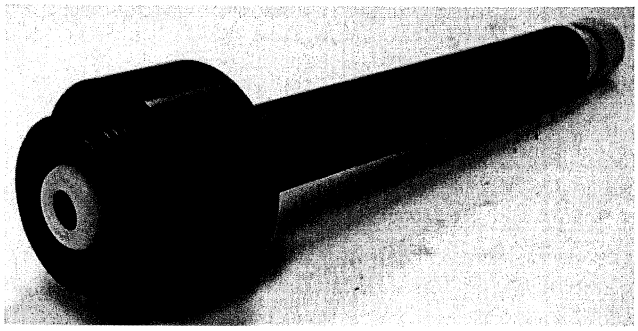

Figure 5-7. Prototype fiber holder.

Another suggestion for a fiber holder is a design with wings, where the fibers are screened off from each other (Figure 5-8). The screening wings eliminate the leaked light between the fibers and would make the Offset measurement unnecessary.

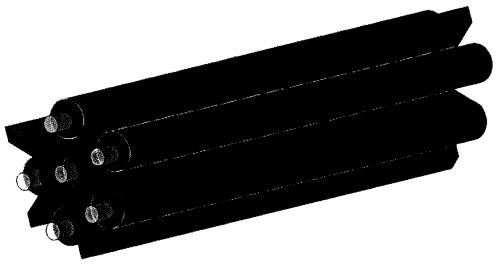

Figure 5-8. Fiber holder with screening wings.

This type of holder will hold six fibers, one in the middle and five between the wings. Constructing a prototype screening holder ourselves was deemed too complicated because of its small size.

5.2. *Programming*

This section briefly describes how the calibration program works. A complete documentation of the program has been written and can be found at SpectraCure AB. Since the software for the main IPDT system is written in LabView, this language was chosen for the Calibration unit as well. LabView (National Instruments, USA) is a graphic programming language directed towards constructing virtual test and measurement systems by analyzing real communication signals from a variety of hardware equipment.

The core of the program is to control the lasers, rotunda, spectrometer and the photodiode amplifier. A front program (GUI) was developed to control the entire calibration procedure. The calibration program is separate from the IPDT system control program but will later be integrated into it.

5.2.1. Treatment Mode

When calibrating the Treatment Mode the program communicates with the photodiode amplifier (Hamamatsu C9329). Measurements by the photodiode of the incoming laser light are taken in by the program and analyzed. Linear calibration curves relating the laser diodes' drive currents to emitted light power are calculated. First the diagnostic laser emits light and the rotunda rotates to all six positions. Then the rotunda is positioned in Treatment Mode and all treatment lasers emit light one by one. The data is placed in a matrix and saved to a file.

5.2.2. Diagnostic Mode

When performing the Offset measurement one fiber emits the diagnostic laser light and the other fibers detect the leaked part. The spectrometer gives a reading of the detected light. The sled is then moved to the Diffuser measurement and the program repeats the procedure of the Offset measurement. The data from the Offset and Diffuse measurements are analyzed and a table of relative losses for each diagnostic laser – fiber combination is made. The table is saved to a file. This table is used in the Diagnostic Mode during a treatment session to adjust the measured data according to each fiber combination's specific losses.

6. Prototype evaluation

This chapter deals with our evaluation work done on the prototype delivered by Akademiska Verkstaden, Sweden, who was hired to build the prototype according to provided designs.

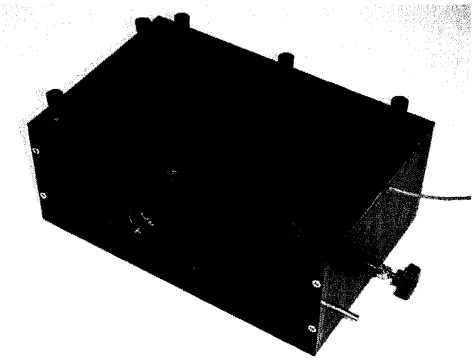

Figure 6-1. Photo of the first IPDT Calibration Unit prototype.

6.1. *Experimental results*

Figure 6-2 shows the setup. A PC sits on top of the IPDT system. The Calibration unit with the fiber holder attached is seen to the right with the Hamamatsu photodiode amplifier to its left.

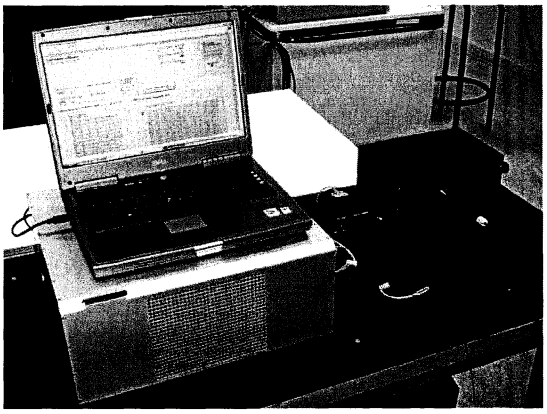

Figure 6-2. Evaluation system setup.

Figure 6-3 shows the interior of the Calibration unit. The sled is in Station 2, with the photodiode ready to measure the light power from the fibers inside the fiber bundle holder. The reflector unit is seen as sharp white, partly blocked by the reflector blocker plate.

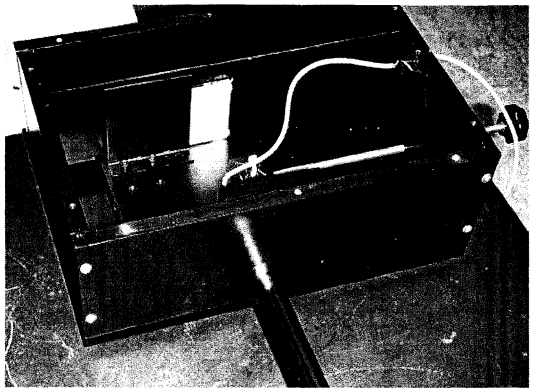

Figure 6-3. Calibration unit without lid. Fiber bundle holder is attached.

6.1.1. Photodiode light cone acceptance

All light exiting the fibers must fit onto the photodiode to calibrate the treatment lasers. To analyze the uniformity of the detection ability of the photodiode a fiber, emitting light, was translated across the detecting area of the photodiode. The fiber's initial position was 10 mm from the center of the photodiode. The fiber tip was always 1 mm from the ND-filter. The results are shown in Figure 6-4.

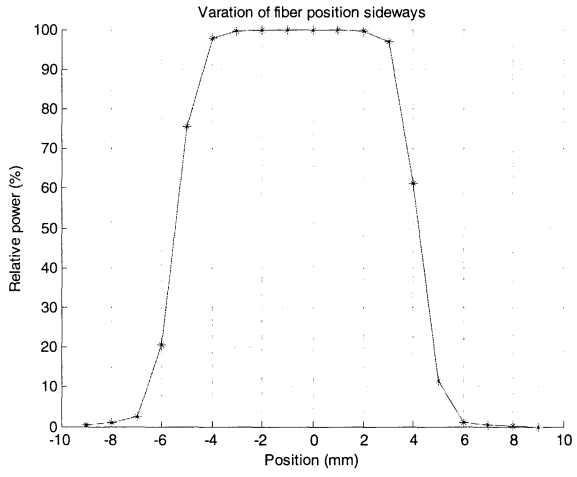

Figure 6-4. Relative detected power as function of position across the photodiode.

It is seen that the photodiode detects the same power (100%) for all fibers placed inside a diameter of 5 mm centered over the photodiode. Since one fiber has the diameter 0.8 mm approximately 6 fibers would fit side by side in front of the photodiode. The detector area is circular

which implies that more than 18 fibers could be used at the same time. This demands that positioning of the fiber bundle is done properly so that all fibers are placed within a diameter of 5mm.

6.1.2. Diffuse reflectance uniformity

The diffuse reflectance was measured for the three distances to the reflector unit (10, 12 and 14 cm), see Figure 6-5. The measurements were done for three different power levels, called power level 50, 70 and 90 in the same way as in 4.2.5.2. The levels correspond to 6, 28 and 49 mW respectively.

The diffuse reflectance can be seen in Appendix B, page B-1. As expected the detected power is higher for position 1 than for position 3 or 4 where it is almost constant, due to lower leakage.

To compensate for the leakage the diffuse reflectance from the reflector blocker was measured (Appendix B, page B-2). The detected power has the same tendency, higher power at position 1 due to more leakage. Note that the detected power for the reflector blocker is much lower than for the reflector unit (mirror and diffuser), as a result of lower reflectance of the reflector blocker.

The compensated results are shown in Appendix B, page B-3. As wanted these are approximately constant for all fiber positions. The deviations, in percent, can be used to more thoroughly examine the light distribution, seen in Appendix B, page B-4. For distances 10 and 12 cm the uniformity seem to be within ±1% excluding position 4. Distance 14 cm shows too large deviation and is thus not a suitable distance.

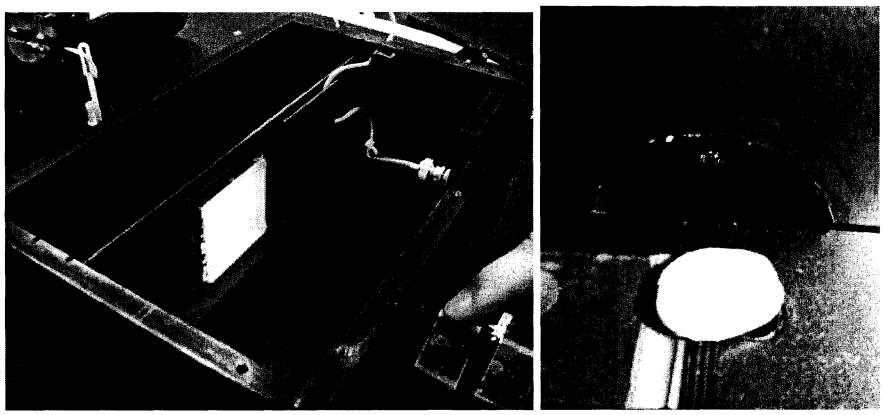

Figure 6-5. Diffuse reflectance test. Fibers are put next to each other in the aperture (without fiber holder). Detecting fiber is moved from position to position.

6.1.2.1. Light leakage

To really control that the light leakage correction worked as expected, the emitting fiber was screened from the other fibers to get a reading with absolutely no light leaking sideways. Measurements were

performed for the distance 12 cm to the reflector unit. The screened measurements were then compared to the compensated values used above, for the same distance (Figure 6-6).

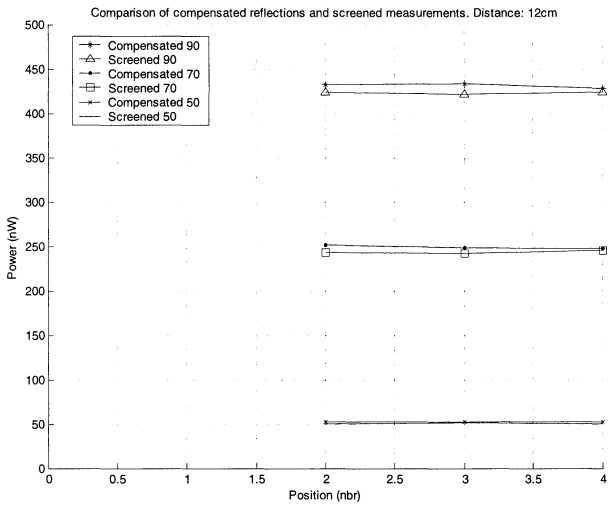

Figure 6-6. Screened measurements compared to calculated compensated values.

The compensated values are a bit higher than the screened measurements. For power level 90 the mean difference is about 2% between the screened and compensated measurements, while it is 2.5% for power level 70 and approximately 4% for power level 50. The screening material could have affected the measurements. Despite these minor differences it is evident that the reflector blocking method can be used to compensate for the leakage between fibers.

6.1.2.2. Reflector blocker material

Two different materials were tested. The material mounted in the housing is black anodized aluminum. The other material was black paper, used in the development process. Measurements were made for the distance 12 cm and all three power levels. Figure 6-7 shows the resulting comparison.

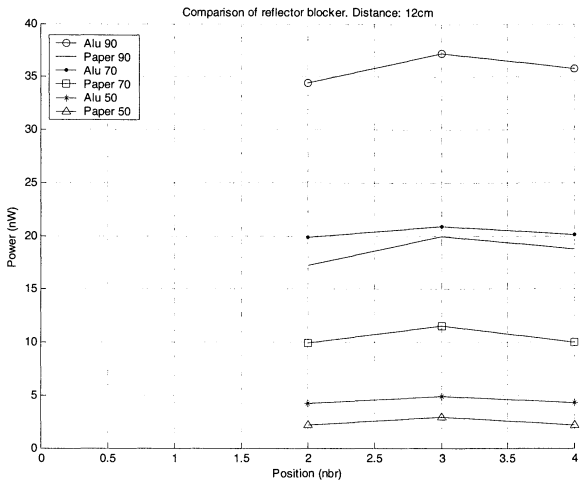

Figure 6-7. Detected power from two reflector blockers made of different materials.

As seen in Figure 6-7 paper is reflecting approximately 50% of what the aluminum reflects. Important properties of the reflector blocker are uniformity of the reflected light and low reflectance.

6.1.2.3. Fiber alignment

To test the influence of variations in fiber alignment the following test was made. For the distance 12 cm and power level 90 the reflected power was detected by a fiber that was misaligned relative the emitting fiber, see Figure 6-8.

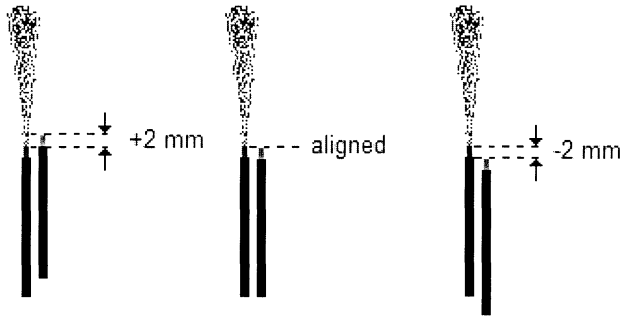

Figure 6-8. Misalignment of fiber during measurements.

The results are shown in Figure 6-9. For uncompensated data, see Appendix B, page B-5.

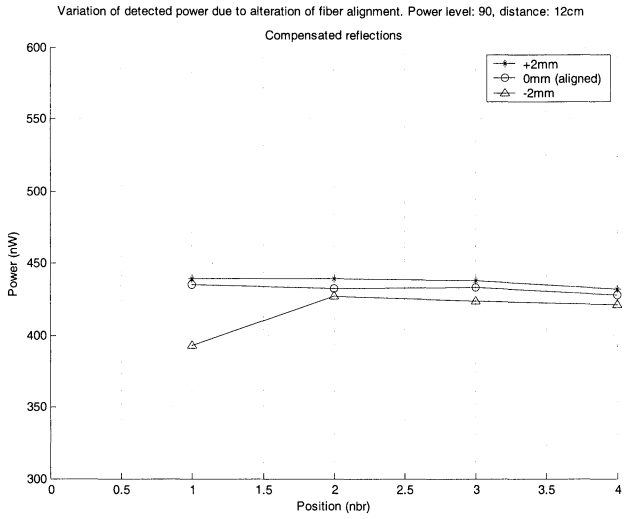

Figure 6-9. Compensated detected power for misaligned fiber.

The resulting compensated values do not differ much when the detecting fiber is in front of the emitting fiber. The large deviation occurring when the detecting fiber is behind the emitting fiber is most likely caused by decreased leakage due to the absorbing jacket of the emitting fiber.

6.2. *Calibration session*

A complete calibration procedure was performed, using six optical fibers coupled to the IPDT system and the Calibration unit. The calibration curves for some selected laser diodes are seen in Figure 6-10. To make sure the photodiode in the Calibration unit functioned correctly, a comparison with an external power meter was performed. As seen in Figure 6-11, the power meter and the photodiode gave an equal linear response to increasing laser diode power. Prior to the measurements the photodiode was calibrated so that the voltage could be related to the correct laser power.

The calibration of Diagnostic Mode resulted in a table of specific fiber losses (see Table 6-1).

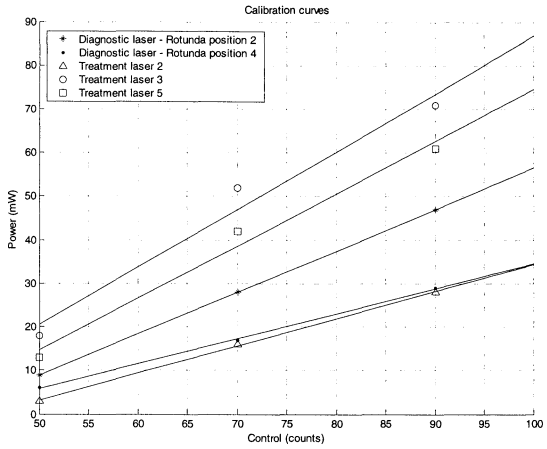

Figure 6-10. Calibration curves for the diagnostic laser diode and three treatment laser diodes.

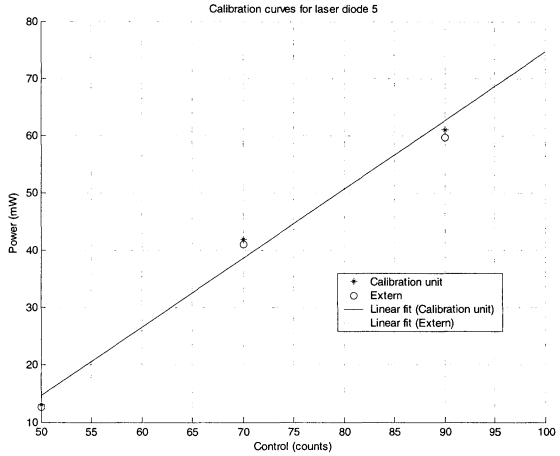

Figure 6-11. Calibration curves for laser diode 5. Both the photodiode in the Calibration unit and an external power meter.

Fiber 1	Fiber 2	Fiber 3	Fiber 4	Fiber 5	Fiber 6
0	1	1.08	0.49	0.83	0.76
1	0.74	1.11	0.41	0.78	0
1.64	1.68	1.99	0.67	0	1
1.67	1.39	1.59	0	1	0.78
2.82	2.40	0	1	1.60	1.57
1.01	0	1	0.35	0.78	0.62

Table 6-1. Fiber losses for all fiber combinations. The values are calculated mean values from measurements with three power levels.

The value zero for a fiber in Table 6-1 means that light is emitted by the fiber. When fiber 1 is emitting all losses are related to fiber 2 hence the value one is inserted for fiber 2. As seen in the table fiber 4 only detects 49% relative fiber 2. In relation to fiber 1, fiber 4 detects only 41%.

7. Discussion

This work presents a simple and cost-effective alternative for a calibration unit, to be used with the SpectraCure IPDT system.

The tests have shown that the calibration can be done for six fibers. The major restrictions in adding more fibers are the detector area of the photodiode and the uniform irradiance from the reflector unit. The evaluation showed that the irradiance was uniform but the deviation increased some in the outer positions. The photodiode has a large detector area but because of the ND-filter, the minimum distance to the detector is increased. The photodiode would however be able to detect all light from a bundle with a diameter of five mm, enabling the bundle to hold more than eighteen fibers.

If a fiber tip is damaged to such a degree that the light exits at extreme angles all light would not hit the photodiode. An integrating sphere would collect all light and might be a more robust solution in the end. Because of its high cost it was not implemented.

The reflector blocker was developed only for compensating the measurements from the leaked light. The materials tested proved to be sufficient although a lower reflecting coating would definitely make the compensation better.

The fiber bundle's alignment in the aperture of the prototype is essential. A fiber holder was developed for minimizing the deviations of fiber placement. The holder is only a first suggestion and should be further developed to possess more user-friendly properties.

The implemented calibration alternative is a relative calibration method. Due to today's patient treatment evaluation the relative calibration method would be enough, although an absolute calibration method yields even more information. This information could be used to extend the analysis of the monitored values.

To assure correct output power calibration the photodiode has to be calibrated. This is done with an external power meter.

We aimed for a simple, user-friendly and functional calibration unit and we claim that the goal is achieved.

8. Future work

This project was only a first study of possible alternatives for the calibration procedure. If our prototype and its underlying principles are deemed stable enough, a similar version will later be developed by a product development consulting company. In the end, a calibration unit would probably be integrated into the IPDT system itself.

It should be possible to develop a smaller version of the calibration unit and still use the same principles of calibration. A rotating wheel carrying a photodiode and the reflector blocker could make the unit more compact. A better way to connect the fiber bundle holder to the Calibration unit should also be developed.

A new photodiode amplifier would probably be constructed to better accommodate the calibration unit's requirements. The Hamamatsu C9329 amplifier used here is too easily saturated.

The Calibration unit might be further developed to also incorporate absolute calibration. This could be done using a photodiode on the inside of the prototype.

Another alternative is an external fiber coupling where two fibers are connected separated by a diffuse material. A known diffuse irradiance is achieved when one fiber emits light and the other detects. If the relative calibration measurements are related to these two fibers the absolute calibration curves can be achieved.

9. Acknowledgements

The guidance and knowledge received from our supervisors Ann Johansson and Thomas Johansson has been greatly appreciated and an essential part of this project.

Thanks to our professor Stefan Andersson-Engels for the opportunity of doing this diploma work and insightful feedback.

The people at the division should be greatly acknowledged for contributing to a pleasant work environment during our project.

Thanks to the people at Akademiska Verkstaden for building our prototype and Katarina Svanberg and Nils Bendsoe for their consultation in clinical guidelines.

Finally we'd like to thank Kerstin Jakobsson for the close cooperation with SpectraCure AB.

10. References

1. T. J. Vogl, K. Eichler, M. G. Mack, S. Zangos, C. Herzog, A. Thalhammer, and K. Engelmann, "Interstitial photodynamic laser therapy in interventional oncology," Eur. Radiol. **14**, 1063-1073 (2004).

2. I. J. MacDonald and T. J. Dougherty, "Basic principles of photodynamic therapy," J. Porphyrins Phthalocyanines **5**, 105-129 (2001).

3. S. G. Bown, "Phototherapy of tumours," World J. Surg. **7**, 700-709 (1983).

4. K. R. Weishaupt, C. J. Gomer, and T. J. Dougherty, "Identification of singlet oxygen as the cytotoxic agent in photo-inactivation of a murine tumor," Cancer Res. **36**, 2326-2329 (1976).

5. C. Eker, "Optical characterization of tissue for medical diagnostics," PhD Dissertation thesis (Lund Institute of Technology, Lund, Sweden, 1999).

6. S. Svanberg, *Atomic and Molecular Spectroscopy – Basic Aspects and Practical Applications*, (Springer Verlag, Heidelberg, Germany, 2003).

7. C. af Klinteberg, "On the use of light for the characterization and treatment of malignant tumours," PhD Dissertation thesis (Lund Institute of Technology, Lund, Sweden, 1999).

8. A. M. K. Enejder, "Light scattering and absorption in tissue - models and measurements," PhD Dissertation thesis (Lund Institute of Technology, Lund, Sweden, 1997).

9. R. Ackroyd, C. Kelty, N. Brown, and M. Reed, "The history of photodetection and photodynamic therapy," Photochem. Photobiol. **74**, 656-669 (2001).

10. I. Wang, S. Andersson-Engels, G. E. Nilsson, K. Wårdell, and K. Svanberg, "Superficial blood flow following photodynamic therapy of malignant skin tumours measured by laser Doppler perfusion imaging," Br. J. Dermatol. **136**, 184-189 (1997).

11. V. H. Fingar, "Vascular effects of photodynamic therapy," J. Clin. Laser Med. Surg. **14**, 323-328 (1996).

12. I. A. Boere, D. J. Robinson, H. S. de Bruijn, J. van den Boogert, H. W. Tilanus, H. J. C. M. Sterenborg, and R. W. F. de Bruin, "Monitoring in situ dosimetry and protoporphyrin IX fluorescence photobleaching in the normal rat esophagus during 5-aminolevulinic acid photodynamic therapy," Photochem. Photobiol. **78**, 271-2 (2003).

13. I. Wang, "Photodynamic therapy and laser-based diagnostic studies of malignant tumours," PhD Dissertation thesis (Lund University, Lund, Sweden, 1999).

14. M. Soto Thompson, A. Johansson, T. Johansson, S. Andersson-Engels, N. Bendsoe, K. Svanberg, and S. Svanberg, are preparing a manuscript to be called "Clinical system for interstitial photodynamic therapy with combined on-line dosimetry measurements."

15. S. Andersson-Engels, N. Bendsoe, T. Johansson, S. Pålsson, M. Soto Thompson, U. Stenram, K. Svanberg, and S. Svanberg, "Integrated system for interstitial photodynamic therapy," in *Advanced Optical Devices,* J. Spigulis, J. Teteris, M. Ozolinsh, and A. Lusis, eds., Proc. SPIE **5123**, 293-302 (2003).

16. S. Svanberg, S. Andersson-Engels, and K. Svanberg. "Divider for distributing radiation.", Patent: SE 503 408. 11-14-2001. Sweden.

17. U. Utzinger and R. R. Richards-Kortum, "Fiber optic probes for biomedical optical spectroscopy," J. Biomedical Optics **8**, 121-147 (2003).

18. A. J. Welch and M. J. C. van Gemert, *Optical-Thermal Response of Laser-Irradiated Tissue*, (Plenum Press, New York, NY, 1995).

19. "Tabulated Molar Extinction Coefficient for Hemoglobin in Water," Oregon Medical Laser Center . (2003), http://omlc.ogi.edu/spectra/hemoglobin/summary.html

20. Inc. LabSphere. "A Guide to Integrating Sphere Theory and Applications," http://www.labsphere.com/uploadDocs/A Guide to Integrating Sphere Theory and Applications_kb100.pdf . (2004),

21. R. Cubeddu, A. Pifferi, P. Taroni, A. Torricelli, and G. Valentini, "A solid tissue phantom for photon migration studies," Phys. Med. Biol. **42**, 1971-1979 (1997).

22. Toshiba. "TLRMH156P LED spec," http://www.semicon.toshiba.co.jp/td/en/Opto/Visible_LED/en_20021217_TLRMH156P_datasheet.pdf . (2004),

23. O. Svelto, *Principles of Lasers*, (Plenum, 1998).

24. J. Envall, P. Karha, and E. Ikonen, "Measurements of fibre optic power using photodiodes with and without an integrating sphere," Metrologia **41**, 353-358 (2004).

25. F. L. Pedrotti and S. J. L. S. Pedrotti, *Introduction to Optics*, (Prentice Hall, Inc., Upper Saddle River, New Jersey, 1996).

26. J. P. A. Marijnissen and W. M. Star, "Calibration of isotropic light dosimetry probes based on scattering bulbs in clear media," Phys. Med. Biol. **41**, 1191-1208 (1996).

Appendix A

Radiometric definitions

Radiance

The radiance L [W/m^{2}sr], at a given point (**r**) for a given direction (**s**), is the radiant power per unit area perpendicular to **s** for a given direction.

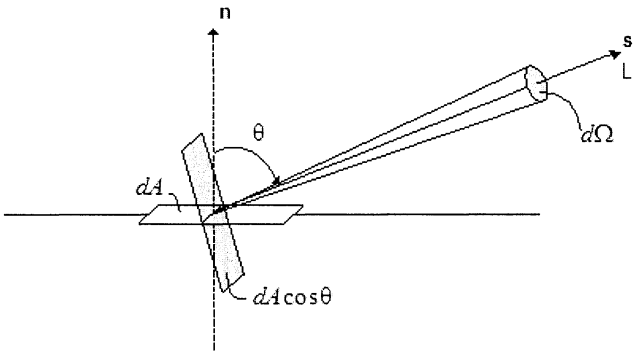

Figure A-1. Radiance [25]

Fluence rate

The fluence rate φ [W/m^2], at a given point in space (**r**), is the radiant power incident on a small sphere divided by the sphere's cross-section.

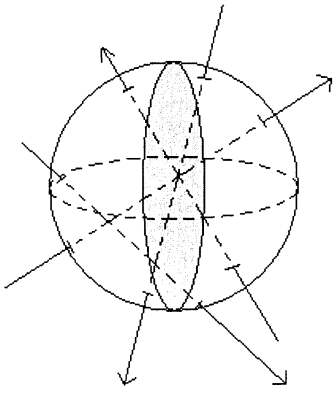

Figure A-2. Fluence rate [26].

The fluence rate is related to the radiance by

$$\varphi(r) = \int_{4\pi} L(r,s)\,d\Omega \qquad \textit{Equation A-1}$$

where $d\Omega$ is an element of solid angle about **s**.

Interstitially inserted optical fibers will only collect a fraction of the fluence rate, due to the fiber acceptance angle. Despite this the fluence rate is, in this thesis, referred to as the detected quantity when collecting light by interstitially inserted optical fibers.

Radiant power

The radiant power P [W] is the power emitted, transferred or received as radiation. The power is related to the radiance by

$$P = \int_{4\pi} \int_{0}^{\pi/2} L(r,s) \cdot \cos\theta \, dA \, d\Omega \qquad \textit{Equation A-2}$$

Radiant intensity

The radiant intensity I [W/sr] in a given direction from a source is the radiant power leaving the source in an element of solid angle containing that element, see Figure A-3.

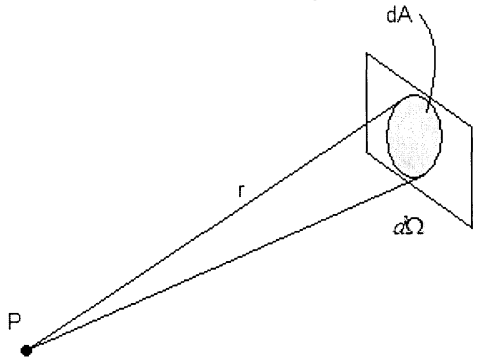

Figure A-3. Point source with radiant power P, incident on an element of area dA with the solid angle dΩ.[25]

The radiant intensity is related to the radiant power by

$$I = \frac{dP}{d\Omega} \qquad \textit{Equation A-3}$$

Irradiance

The radiant power incident onto a surface is called irradiance, E [W/m^2], see Figure A-3.[25]

The irradiance is related to the radiant power by

$$E = \frac{dP}{dA} \qquad \textit{Equation A-4}$$

Appendix B

Prototype evaluation measurement results

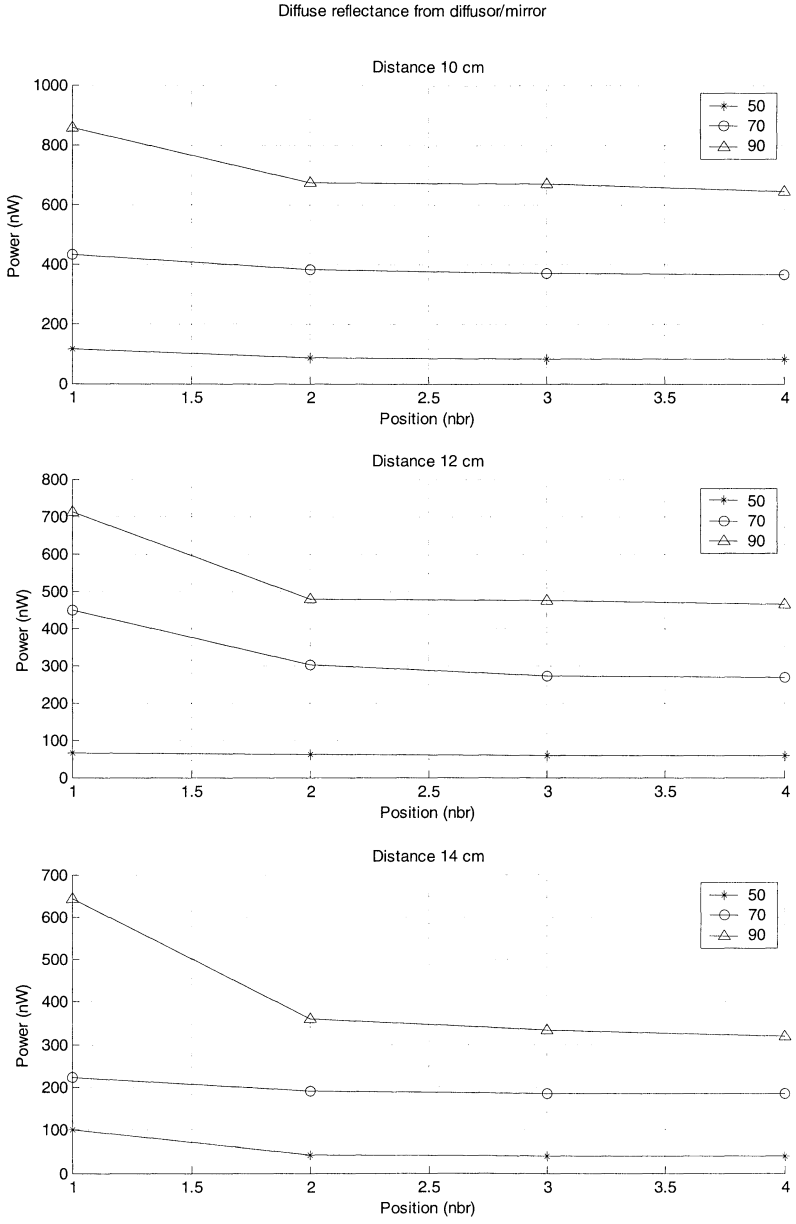

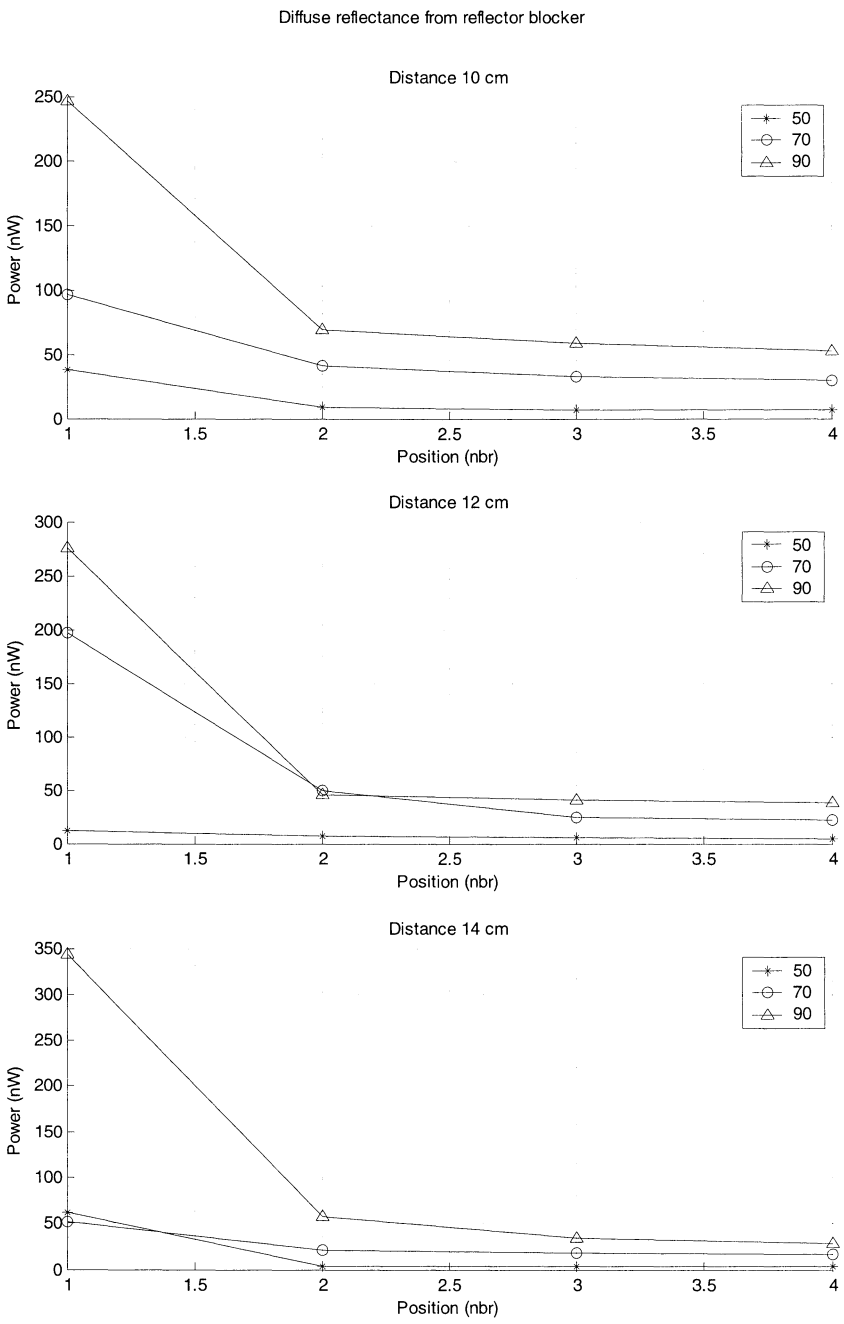
Diffuse reflectance from reflector blocker
Distance 10 cm
Power (nW)
Position (nbr)
50
70
90
Distance 12 cm
Power (nW)
Position (nbr)
50
70
90
Distance 14 cm
Power (nW)
Position (nbr)
50
70
90

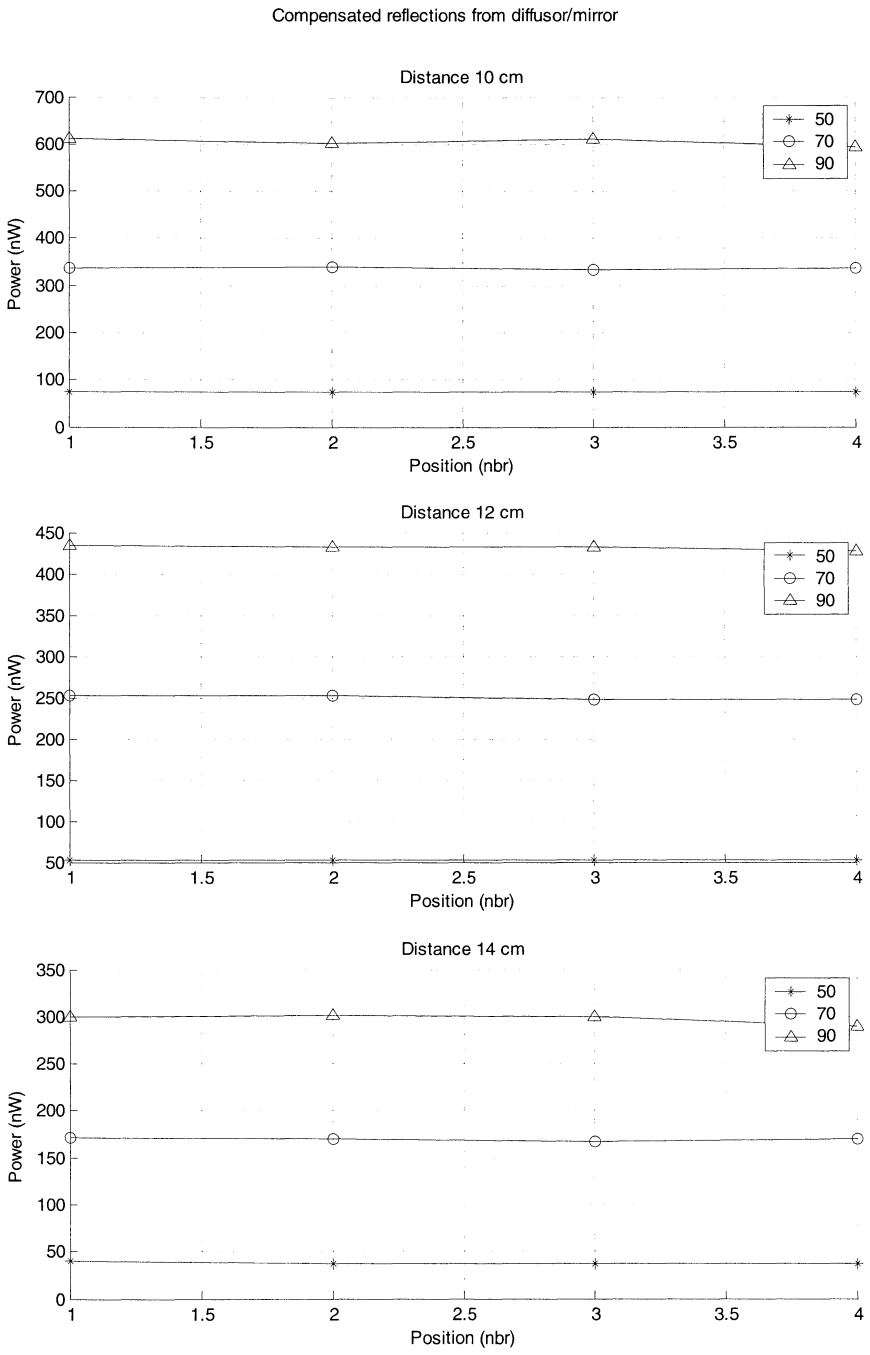
Compensated reflections from diffusor/mirror
Distance 10 cm
Power (nW)
Position (nbr)
50
70
90
Distance 12 cm
Power (nW)
Position (nbr)
50
70
90
Distance 14 cm
Power (nW)
Position (nbr)
50
70
90

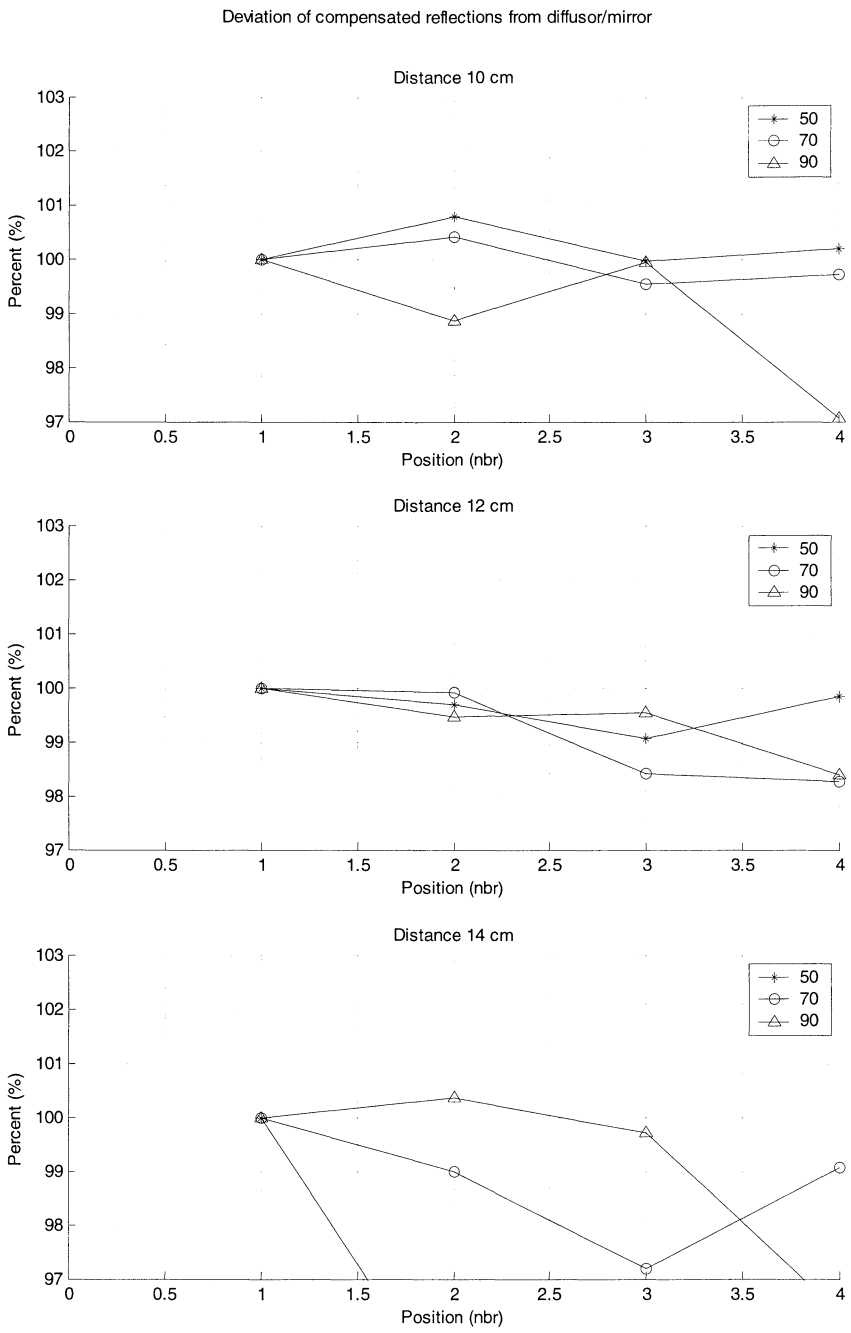
Deviation of compensated reflections from diffusor/mirror
Distance 10 cm
Distance 12 cm
Distance 14 cm
50
70
90
Percent (%)
Position (nbr)
103
102
101
100
99
98
97
0
0.5
1
1.5
2
2.5
3
3.5
4

Variation of detected power due to alteration of fiber alignment. Power level: 90, distance: 12cm